Geol. Mag.: page 1 of 30 © Cambridge University Press 2016
doi:10.1017/S0016756816000339

Reactivation, inversion and basement faulting and thrusting in the Sierras Pampeanas of Córdoba (Argentina) during Andean flat-slab deformation

ROBERTO D. MARTINO*, ALINA B. GUERESCHI & ANA CARO MONTERO

Departamento de Geología Básica, Facultad de Ciencias Exactas, Físicas y Naturales, Universidad Nacional de Córdoba (UNC), CICTERRA (CONICET–UNC) and CIGEA (UNC–CNEA), Córdoba, Argentina

(*Received* 30 October 2015; *accepted* 25 March 2016)

Abstract – The Sierras Pampeanas of Córdoba are the easternmost uplifted blocks caused by Andean foreland deformation, over 700 km from the Chile trench. This deformation started at *c.* 340 Ma through basement faults, thrusts and reactivation of normal faults of the Cretaceous rift during the opening of the Atlantic Ocean. Other older faults, major oblique lineaments, were also reactivated. Thermochronological and geothermobarometric data indicate that some topographic relief could have been Palaeozoic–Mesozoic relicts and not only produced by the Andean orogeny. Faults are partially controlled by the early Cambrian S_2 metamorphic foliation, coincident with the curved fault traces at map scale. During Pliocene time, two deformation phases post-dating Miocene–Pliocene magmatism are recognized. Shallow seismicity data (*c.* 25 km depth) indicate that the Sierras de Córdoba accommodate Quaternary displacement. Magnetotelluric studies detect the interface between the Pampia terrane and the Río de la Plata craton. The role of the oblique lineaments in the nucleation and development of the Tertiary faulting has been little considered; they could be correlated with an old pan-Gondwanan trend. During the Cretaceous period these lineaments worked in a transtensive way, producing the uplift of high-grade rocks and segmentation of the mountain chain favouring the diachronous uplift along the ranges. Recently, both the brittle–ductile transition at *c.* 23 km depth and the crustal thickness have been determined by seismicity analysis. The oblique lineaments displace normally the Mohorovicic discontinuity. Main basement thrusts were probably rooted in the suture between the Pampia terrane and the Río de la Plata craton.

Keywords: thick-skinned style, faulting, lineaments, Andean deformation, Eastern Sierras Pampeanas.

1. Introduction

The continental lithosphere of the southwestern part of the Gondwana supercontinent was consolidated towards the end of Proterozoic time (for details, see Ramos, 1988; Ramos, Cristallini & Pérez, 2000). This process introduced a planar anisotropy in the basement that controlled the development of Phanerozoic basins in Argentina. The accretion of terranes to the Pacific margin of Gondwana during the early Palaeozoic era reactivated these anisotropies and created others, mainly during the Ordovician–Silurian periods (Ocloyic deformation phase). Mesozoic basins with two extensional styles were accommodated by NE and NW planar structural fabrics that affected the metamorphic basement in the Río de la Plata and Pampean domains, facing the Atlantic and Pacific continental margins, respectively (Fig. 1; Martino, Guereschi & Carignano, 2012).

In the Pampean domain, two lineaments that controlled the Cretaceous basins in the central mainland of Argentina (Fig. 1) are recognized: the Valle Fértil lineament; and the Eastern Pampean lineament. The latter is reactivated today and forms the current Sierra Chica fault in the Eastern Sierras Pampeanas (Uliana, Biddle & Cerdan, 1989; Rossello & Mozetic, 1999; Chebli *et al*. 2005; Richardson *et al*. 2009). These two lineaments are sutures: the Valle Fértil lineament is the Palaeozoic suture marking accretion of the Cuyania terrane (Precordillera plus Western Sierras Pampeanas; Ramos *et al.* 1986) to the Pacific Gondwana margin; and the Eastern Pampean lineament is the suture assembly of the Río de la Plata craton with the Pampia terrane in Precambrian times.

Tertiary Andean compression, recording arrival of the Nazca plate with low-angle subduction, produced inversion of Cretaceous basins (Schmidt *et al*. 1995), block-faulting and clockwise-tilting (relative to present-day north), resulting in the current landscape of the Sierras de Córdoba (Gordillo & Lencinas, 1979). The uplift of these blocks and the landscape of tilted blocks impressed one of the first geologists who systematically studied the Argentinian territory (Stelzner, 1875). The natives called the high plains 'pampas' and, because of the common appearance of the 'sierras' and 'pampas' landscape, Stelzner gave these ranges the name 'Pampinas' which became 'Pampeanas'.

The Sierras de Córdoba are the easternmost group of the Sierras Pampeanas geological province. They consist of a Neoproterozoic–Palaeozoic basement arranged

*Author for correspondence: roberto.martino@unc.edu.ar

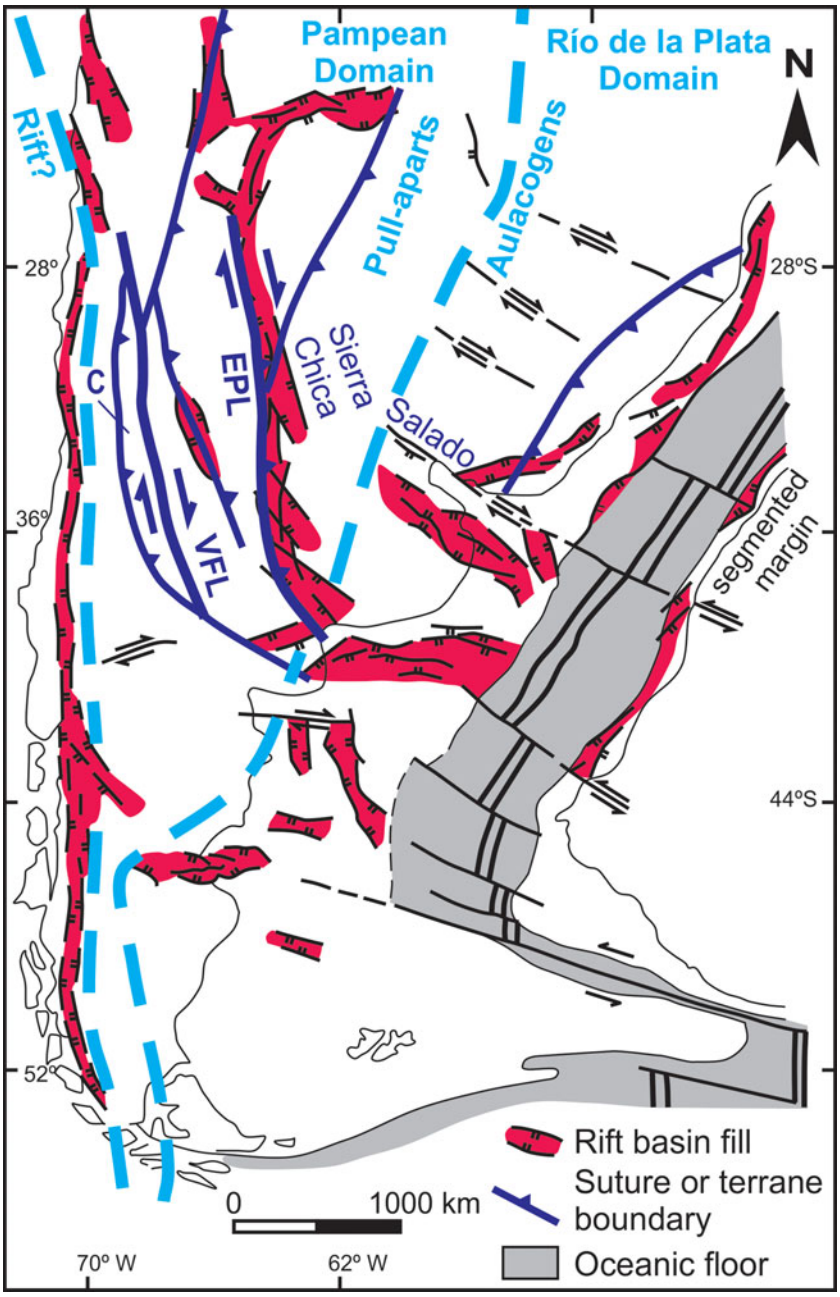

Figure 1. (Colour online) Schematic map of southern South America showing the Mesozoic extensional basins in Argentina (modified from Uliana, Biddle & Cerdan, 1989; Rossello & Mozetic, 1999; Chebli *et al*. 2005; Martino *et al*. 2014). These are accomodated on structural planar fabrics orientated NW and NE, affecting the metamorphic basement in the Pampean and Río de la Plata domains (separated here by the dashed line). In the Pampean domain, two lineaments that controlled the Cretaceous basins are recognized – the Valle Fértil lineament (VFL) and the Eastern Pampean lineament (EPL) – today reactivated and forming the Sierra Chica fault. These two lineaments correspond respectively to two sutures, the Palaeozoic accretion of Cuyania (C) to the Pacific Gondwana margin (VFL) and the assembly of the Río de la Plata craton with the Pampia terrane in Precambrian times (EPL). The latter and the Sierra Chica fault are probably the surface expression of the true suture which is situated towards the east at lower structural levels of the lithosphere, where it has been geophysically detected.

in N–S-aligned mountain ranges, limited by Tertiary W-vergent reverse faults and thrusts (Fig. 2).

A first version of the Tertiary structure of the Sierras de Córdoba was a sketch published by Beder (1922), reproduced here as Figure 3. The first to address the problem of block uplift was González Bonorino (1950). In a pioneering work this author suggested that the uplift faults, reflecting shallow brittle deformation as a result of compression, would become horizontal at depth: plastic deformation absorbs brittle deformation and the upper crust would be displaced in the lower crust along roughly horizontal planes, anticipating the concept of brittle–ductile transition applied to lithospheric deformation. Cuerda (1973) applied the concept of 'pillar-bridge horse' to the sinking towards the ends of the raised blocks, with maximum displacement in their central parts.

Figure 2. (Colour online) (a) Panoramic view to the ENE of the Sierras Pampeanas of Córdoba. The linearity of the mountain ranges separated by reverse faults and basement thrusts are evident. In the foreground, the NW corner of the Achala batholith, Sierra Grande, and in the background, Sierra de Cuniputo and Sierra Chica on the horizon. The point of maximum height is the Cerro Uritorco (1950 m a.s.l.). (b) View toward ESE in the foreground showing the Pampa de Pocho and a small dark range named La Sierrita, composed of mylonitic rocks from the Ambul–Mussi ductile shear zone, with the La Sierrita fault at its foot. Silhouetted against the horizon are the Sierra Grande block and its southwards prolongation into the Sierra de Comechingones. (c) View SE from the central part of the Achala batholith towards the scarp of the Sierra de Comechingones fault. The point of maximum height is the Cerro Champaquí (2884 m a.s.l.). In the central part of the escarpment, it is the horst-like elevation of the Pampa de Achala shown in Figure 9.

Briefly, according to Jordan & Allmendinger (1986) uplift of the basement blocks in the Sierras de Córdoba would have started about 10 Ma ago, but today there is evidence of rising as old as the Carboniferous period (Ramos, 1988; Jordan *et al*. 1989; Coughlin *et al.* 1998; Löbens *et al*. 2011; Martino, Guereschi & Carignano, 2012; Richardson *et al*. 2013). Block uplift could be produced by: (1) low-angle reverse faults (thrusts, Kraemer *et al*. 1988; Kraemer, Escayola & Martino, 1995), modified locally to higher angles by stacking of the underthrusting wedge (Kraemer & Martino, 1993); and (2) reactivation by inversion of high-angle normal faults of the Cretaceous rift (Schmidt *et al*. 1995). Other older faults oblique to the current dominant trend (probably related to a pan-Gondwanan trend; Daly, 1988; Tankard *et al*. 1995) have also been reactivated. The role of the oblique lineaments has been little considered in the nucleation and development of the Tertiary faulting.

Two main deformational events have been established based on these styles of faulting ((1) new; and (2) reactivation and inversion), using stratigraphic evidence and regional correlation (Martino *et al*. 1995). These occurred at *c.* 2 Ma (event B) and *c.* 0.8 Ma (event A).

Magmatism associated with the Andean orogenic cycle is represented by Tertiary volcanic rocks in the NW margin of the Sierras de Córdoba (Pocho Volcanic Complex, 7.9–4.7 Ma, Kay & Gordillo, 1994; Arnosio *et al*. 2014) and in the Sierra de San Luis (e.g. Sierra del Morro, 2.6 ± 0.7 and 1.9 ± 0.2 Ma; Ramos, Munizaga & Kay, 1991). Quaternary movements are recognized in the El Molino fault near Merlo, and in the Sierra Chica fault (Costa & Vita-Finzi, 1996; Costa *et al*. 2001). Seismological and seismic risk data linked to the latest deformation have recently been reviewed by Fatala & Martino (2012), Perarnau *et al*. (2012), Costa *et al*. (2014) and Caro Montero, Martino & Guereschi

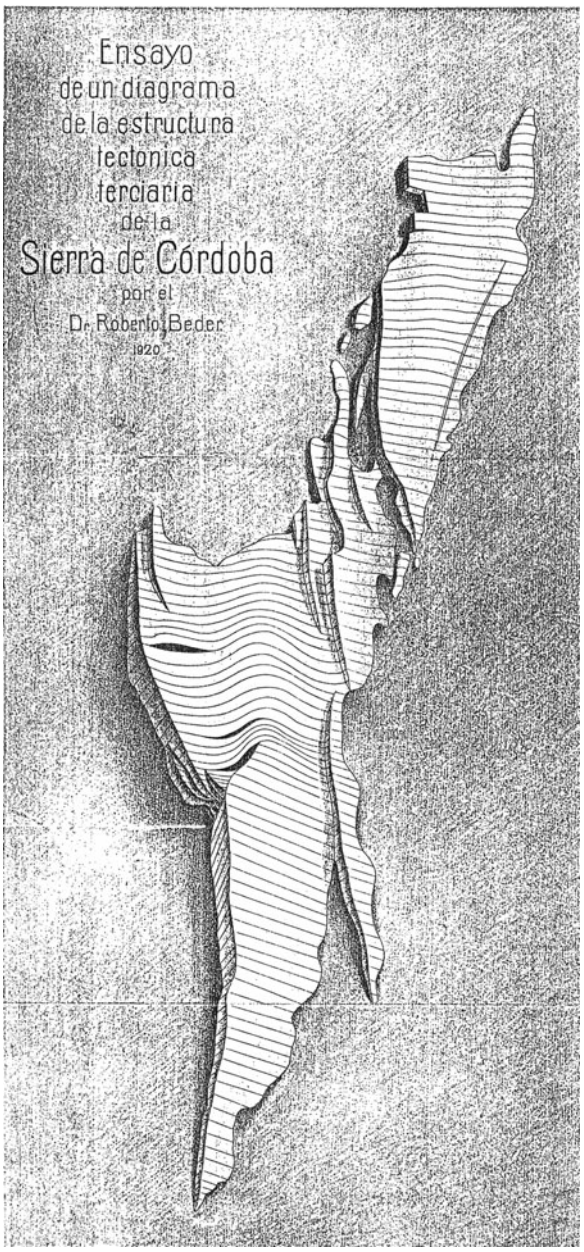

Figure 3. Sketch of the Tertiary tectonic structure (block uplift) of the Sierras de Córdoba published by Beder (1922).

(2015). Richardson *et al*. (2013) evaluated the depth of the Mohorovicic discontinuity and presented (U–Th)/He thermochronometric data from apatite and zircon, which gave ages of Permian – Early Jurassic cooling, suggesting that subsequent exhumation has been less than 2–3 km. An even older age (Carboniferous) has been proposed, so the current relief could have Palaeozoic and Mesozoic relicts and not only have been produced by the Andean orogeny (Jordan *et al*. 1989; Coughlin *et al*. 1998; Löbens *et al*. 2011; Martino, Guereschi & Carignano, 2012).

The objectives of this work are: (1) to describe and interpret the faults and thrusts of the Sierras de Córdoba basement produced during the Andean orogeny; and (2) to evaluate the influence of pre-Andean tectonics in Andean structures. Both objectives are integrated into a synthesis of thick-skinned deformation affecting the Sierras de Córdoba and their tectonic evolution.

2. Geological setting

The Sierras Pampeanas province of central Argentina is a region of large mountain ranges of crystalline basement and intervening broad valleys. The ranges are blocks raised by the deformation of the current Andean foreland, over 700 km from the Chilean trench, coinciding with a sector of low-angle inclination of the Nazca plate beneath the South American plate. The 'flat-slab' geometry of the subducted Nazca plate and the deformation of the upper plate (South American), by coupling between them, have been compared with the Laramide orogeny in North America and elsewhere (Jordan *et al*. 1983*a*, *b*; Rodgers, 1987; Marshak, Karsltrom & Timmons, 2000). The Pampean flat-slab occurs between 27° and 34° S and had existed from 20 Ma to the present (Yañez *et al*. 2001; Ramos, Christallini & Pérez, 2002). In a review, Ramos & Folguera (2009) constrained the activity from 12 Ma to present. Basement deformation (thick-skinned tectonics) affected an area of about 800 × 600 km. The deformation is of Cenozoic age and the mountain ranges were uplifted mainly by reverse faulting and folding locally.

The Sierras de Córdoba are the most eastern group of the Sierras Pampeanas. They consist of a polydeformed metamorphic basement (Gordillo & Lencinas, 1979; Martino & Guereschi, 2014) of Neoproterozoic – early Palaeozoic ages (Rapela *et al*. 1998; Siegesmund *et al*. 2010). The outcropping metamorphic basement is predominantly composed of large migmatitic massifs with minor gneisses, amphibolites and marbles. Pressure and temperature conditions reached granulite facies with anatexis (7–8 kb, 700–800 °C; Guereschi & Martino, 2014). Low-grade rocks crop out only locally, such as phyllites in the western edge of the Sierra de Pocho. The metamorphic basement is affected by a highly penetrative metamorphic foliation called S_2 (Neoproterozoic–Cambrian age), which exerted a strong control on the deformation as many authors have highlighted (Gordillo & Lencinas, 1979; Kraemer *et al*. 1988; Massabie & Szlafsztein, 1991; Kraemer & Martino, 1993; Simpson *et al*. 2001; Martino, Guereschi & Carignano, 2012; Martino *et al*. 2014).

The metamorphic basement was imbricated by contractional ductile shear zones during Ordovician–Silurian and Devonian–Carboniferous times (Martino, 2003; Steenken *et al*. 2010) and intruded by Palaeozoic granitoids (e.g. the Achala batholith; Figs 4, 5).

The metamorphic basement of the Sierras de Córdoba was exhumed by denudation and has remained essentially exposed since middle Palaeozoic time (Ramos, 1988; Simpson *et al*. 2001; Whitmeyer, 2008; Steenken *et al*. 2010; Bense *et al*. 2013). On the western margin of the mountains, minor outcrops of Carboniferous–Permian continental sedimentary rocks are recognized at the foot of the Sierra de Pocho. To the east in the Sierra Chica, Cretaceous continental

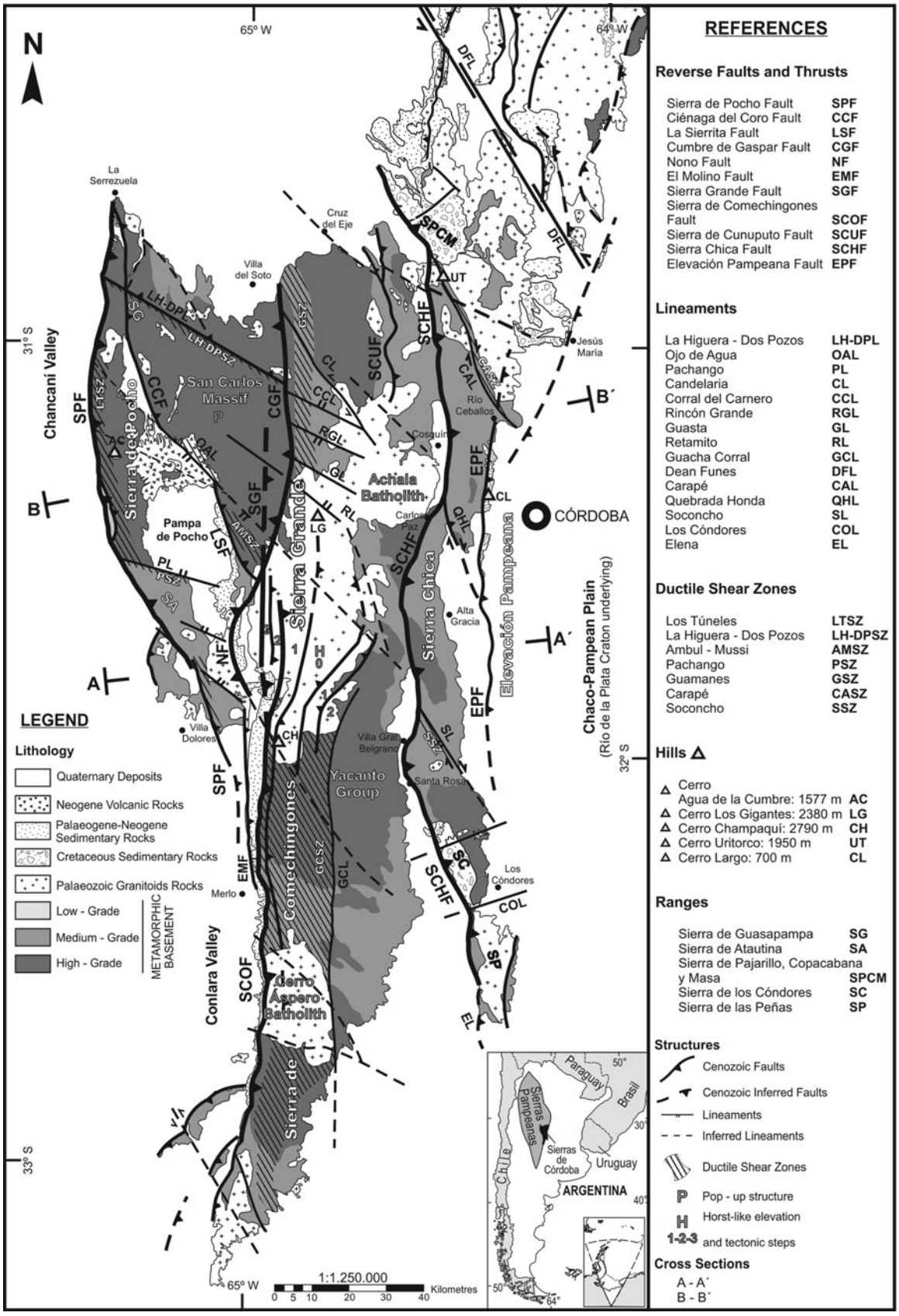

Figure 4. Geological map of the Sierras de Córdoba, showing the traces of the main brittle Cenozoic structures (modified from Martino, Guereschi & Caro Montero, 2014).

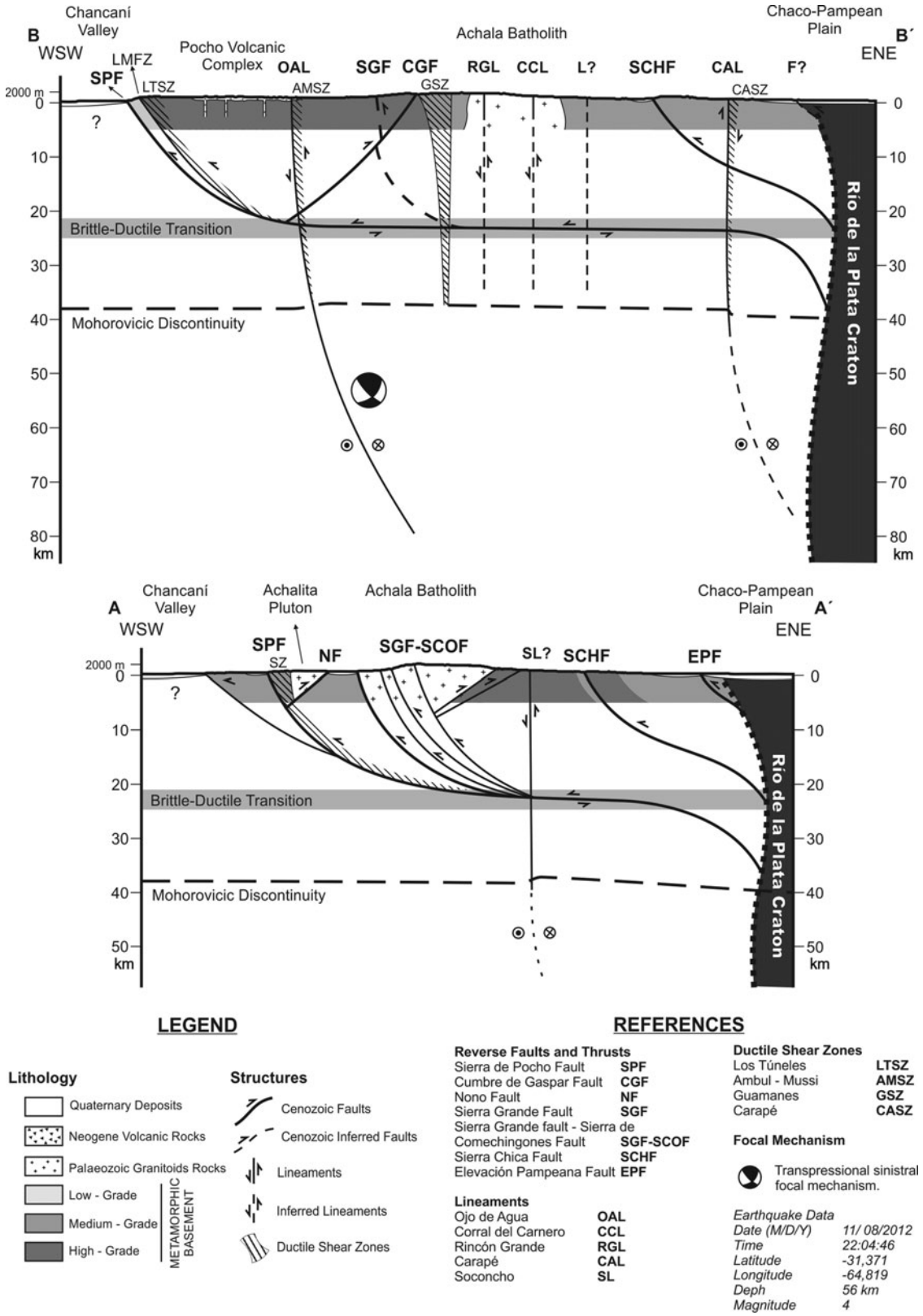

Figure 5. Geological sections A–A′ and B–B′ orientated ESE, crossing the main brittle Cenozoic structures in the Sierras de Córdoba (see Fig. 4 for locations). In addition to the observable surface geology, the main faults and thrusts that uplifted the ranges are represented as interpreted in depth based on geophysical data obtained by Favetto *et al*. (2008), Perarnau *et al*. (2012) and Orozco *et al*. (2013). Focal mechanism calculated by the International Seismological Center (see details in Fig. 14).

sedimentary rocks crop out associated with basaltic flows and dykes (Lagorio, Vizán & Geuna, 2014).

The uplift in asymmetric blocks of the Sierras Pampeanas of Córdoba is arranged in N-striking mountain ranges, limited by Tertiary reverse faults, mainly W-vergent high-angle faults and low-angle faults (thrusts). It has a steep western flank, while the eastern flank is gentle (e.g. 10–12° slope, Sierra Chica). From west to east (Figs 3–5), the ranges are: Sierra de Pocho; Sierra Grande–Sierra de Comechingones; Sierra Chica; and Elevación Pampeana. These mountain ranges are separated by intermountain valleys with Cenozoic continental sedimentary rocks. Palaeogene deposits are scarce, but late Eocene – Oligocene synorogenic deposits in the Sierra Chica are evidence of early uplift (Lencinas & Timonieri, 1968). Neogene deposits are more widespread in the intermountain valleys and foothills, related to major uplift of the mountains in the late Miocene period (Jordan & Allmendinger, 1986). In the northwestern area, Neogene volcanic and pyroclastic rocks (Pocho Volcanic Complex) overlie the landscape of E-tilted blocks. The whole of the Sierras de Córdoba emerges from the Chaco-Pampean plain of Quaternary age, with abundant Mesozoic and Cenozoic deposits in depth.

3. Basement faults and thrusts

A new map with the trace and the interpretation of the main faults and thrusts recognized in the basement of the Sierras Pampeanas of Córdoba is shown in Figure 4.

It should be noted that the term 'fault scarp' is used here in the sense of Stewart & Hancock (1990), who defined it as a matching geoform coincident or grossly coincident with a fault plane that has affected the surface of the ground. This criterion has been used in tracing the faults and thrusts on the map of Figure 4.

The main structures recognized in the Sierras de Córdoba were also traced on satellite images combined with a digital elevation model (Fig. 6). The bow-and-arrow method (Elliot, 1976) was applied to some typical thrusts, measuring the length L of the exposed faults on the map to estimate the maximum displacement D and the tectonic transport direction (see Section 6 below).

From the geological map (Fig. 4), two new sections transverse to the Sierras de Córdoba (Fig. 5) were made. They are representative of the morphology of the brittle Cenozoic tectonics affecting these ranges. In addition to the observable surface geology, the main faults and thrusts that deform and uplift the ranges were represented and interpreted in depth in both sections based on geophysical data obtained by Favetto *et al*. (2008), Perarnau *et al*. (2012) and Orozco *et al*. (2013). Both sections are described and interpreted in Section 7.

Based on seismic activity (databases taken from *Instituto Nacional de Prevención Sísmica* in Argentina, United States Geological Survey and T. Richardson, unpubl PhD thesis, Purdue University, 2011), epicentres and hypocentres of recorded earthquakes are represented in a particularly active area as it is the western zone of section B–B' (Figs 4, 5). From May 1923 to August 2015, a total number of 585 earthquakes were recorded (115 > 40 km depth and 470 < 40 km depth). Two focal mechanisms were obtained from the International Seismological Center. Most of the recorded magnitudes (M_b) vary between 2 and 4 (80 %). Several sections perpendicular to the La Sierrita fault, the Ojo de Agua lineament and the Ciénaga del Coro fault were made. Analysing these sections, hypocentres were interpolated using the Natural Neighbour method. The results are described and interpreted in Sections 4 and 7.

In the following sections, the main faults and thrusts recognized in the basement of the Sierras Pampeanas of Córdoba are described from west to east, from oldest to youngest, following the deduced direction of deformation propagation toward the buttress of the Río de la Plata craton (see Section 6).

3.a. Sierra de Pocho fault

This fault scarp borders a large block that raised the basement *c.* 1000 m above the Chancaní Valley. As a result, from north to south the Sierras de Guasapampa, Pocho and Altautina were formed, describing a large arc convex to the west (Fig. 4). To the south, this fault probably continues parallel to the El Molino fault (Costa *et al*. 2014), covered by modern deposits in the Conlara Valley. The Sierra de Pocho fault is the longest fault in the Sierras Pampeanas; to the north of the Sierras de Córdoba between 26° and 33° S latitudes it extends by almost 700 km, striking *c.* N 350º.

The geological map of the central part of the Sierra de Pocho and a detailed section of this fault is shown in Figure 7a–c. The hangingwall consists of Cambrian metamorphic rocks, such as the La Mermela phyllites and mylonitic rocks of the Los Túneles ductile shear zone (Martino, 2003). The footwall, coincident with the Chancaní Valley, is represented by a large, W-vergent, asymmetric synformal fold (a drag fold?) in Permian–Carboniferous sedimentary rocks, partially covered by modern sediments and profuse vegetation.

The La Mermela phyllites form a lenticular body on the map, limited by the Sierra de Pocho fault to the west and by the La Mermela fault zone to the east, both of reverse-type and brittle regime (Martino, Guereschi & Sfragulla, 2002). On the map, both structures are connected by a rejoining splay (in the terminology of Boyer & Elliot, 1982) which has the 3D shape of a horse fault composed of the La Mermela phyllites (Fig. 7a, b). The La Mermela fault zone produced intense grinding and Fe-loss from biotite in the mylonitic rocks of the Los Túneles shear zone. Tabular cataclasite bands of decimetre thicknesses are recognized (Fig. 7c), consisting of gouge (N 5°/53° E) and breccia (N 350°/75° E) and a strong subhorizontal fracture cleavage (N 305°/30° N).

To the east beyond the La Mermela fault zone the Los Túneles shear zone has brittle deformation superimposed on the ductile deformation, evidenced by minor

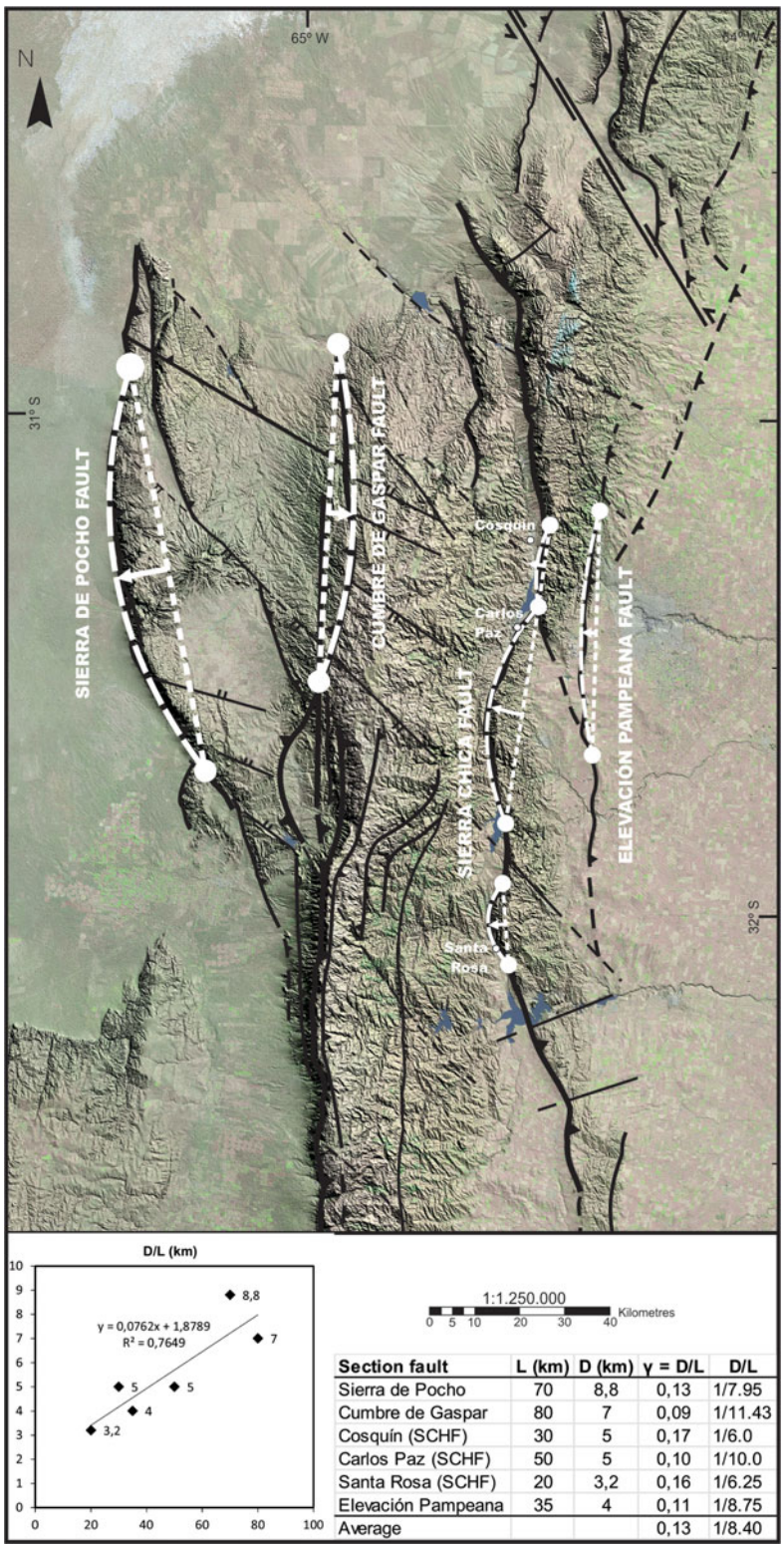

Section fault	L (km)	D (km)	y = D/L	D/L
Sierra de Pocho	70	8,8	0,13	1/7.95
Cumbre de Gaspar	80	7	0,09	1/11.43
Cosquín (SCHF)	30	5	0,17	1/6.0
Carlos Paz (SCHF)	50	5	0,10	1/10.0
Santa Rosa (SCHF)	20	3,2	0,16	1/6.25
Elevación Pampeana	35	4	0,11	1/8.75
Average			0,13	1/8.40

Figure 6. (Colour online) Main traces of thrust faults recognized in the Sierras de Córdoba highlighted on Landsat 7 satellite images, with 8 bands (1–7: resolution 30 m, 8: pancromatic resolution 15 m) from EarthExplorer (http://earthexplorer.usgs.gov/ containing information from https://lta.cr.usgs.gov/LETMP) on a digital elevation model (DEM), resolution 45 m, from the Instituto Geográfico Nacional of Argentina (http://ign.gob.ar/node/987). The bow-and-arrow method (Elliot, 1976) was applied to the main curved, low-angle thrust faults (interpreted here as new Cenozoic faults), measuring the length *L* of the exposed faults on the map, to estimate the maximum displacement *D* and the tectonic transport direction (arrows). The results are displayed in the table and diagram of *D* versus *L* (in kilometres).

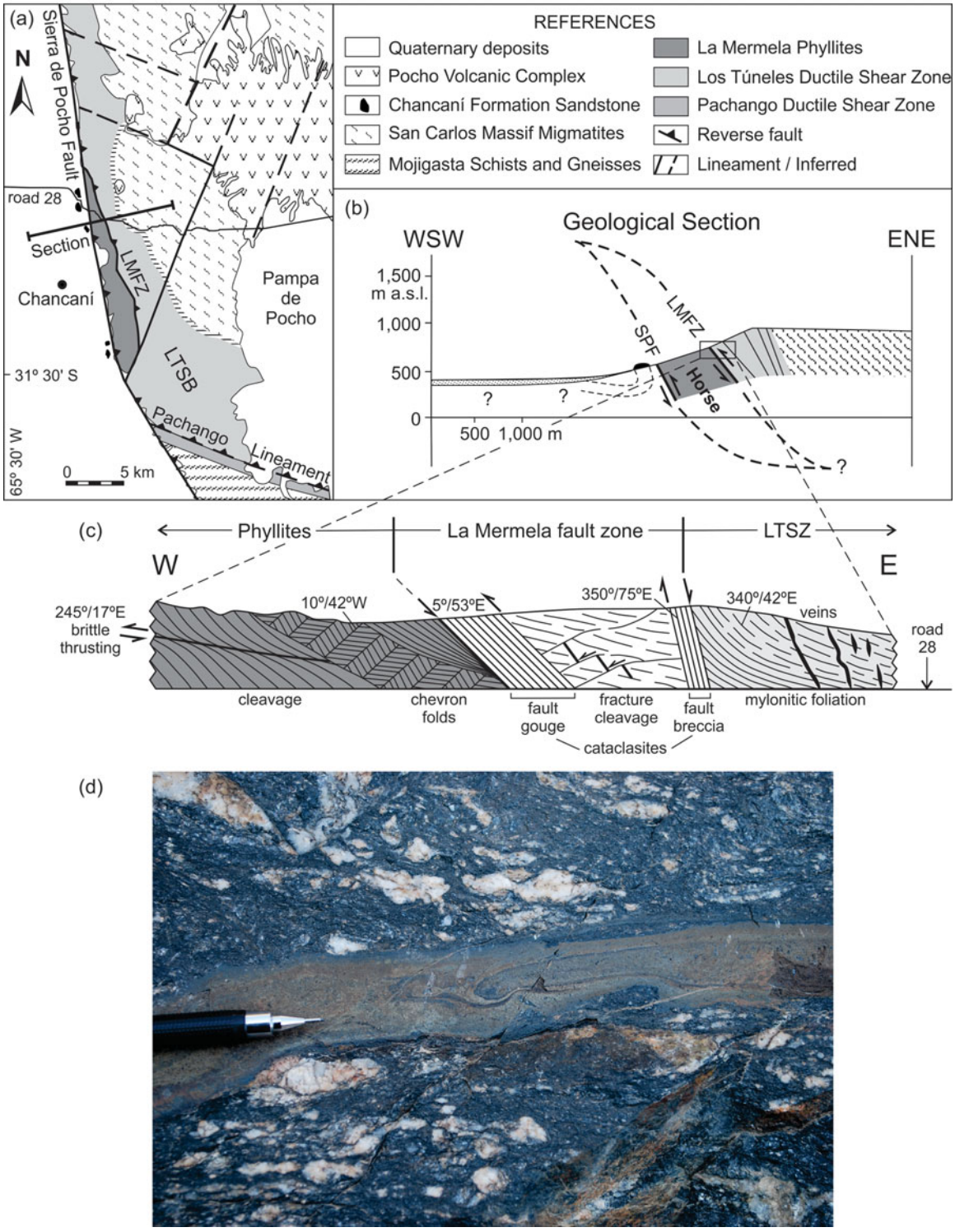

Figure 7. (Colour online) (a) Detailed geological map of the Sierra de Pocho (modified from Martino, Guereschi & Sfragulla, 2002), showing the Sierra of Pocho fault (SPF) and the La Mermela fault zone (LMFZ) connected by a rejoining splay (Boyer & Elliott, 1982). (b) Geological cross-section showing the 3D effect of these structures, forming the horse of the La Mermela phyllites. (c) Detailed geological section of the La Mermela fault zone, at the contact between the Los Túneles ductile shear zone (LTSZ) and the La Mermela phyllites. The reverse LMFZ is nucleated in rocks from LTSZ, producing strong crushing and Fe-loss from biotite. Two tabular sheets of cataclasites of decimetric thickness, consisting of gouge (N 5°/53° E) and a breccia (N 350°/75° E), and a strong subhorizontal fracture cleavage (N 305°/30° N) are also recognized. (d) Photograph showing pseudotachylite veins generated by brittle deformation superimposed on the Los Túneles shear zone, east of the La Mermela fault zone.

conjugated thrusts, cataclasis with pseudotachylite generation (Fig. 7d) and calcite–chlorite veins.

Minor conjugated thrusts (Fig. 8a) are two sets of low-angle faults (<30°): one set strikes N 340–345°, E-dipping by 4–17°, and the other strike N 235–277°, with 15–27° N dip (Martino, Guereschi & Sfragulla, 2002). These thrusts affected both the Los Túneles ductile shear zone and the La Mermela phyllites, cutting the dominant E-dipping foliation in both lithologies but producing different structures depending on the angular relationship between the two planes (α). When the angle between thrusting and foliation was low (α <40°, E-dipping thrusts), drag folds were produced; while when the angle was high (α ≈ 60°, N-dipping thrusts), asymmetric kink-bands, Z-shaped facing north, were generated. The N-dipping thrusts are penetrative and spaced at 1–10 m. Using these conjugates thrusts, the approximate orientations of the axes of shortening $Z =$ N 312°/10°, intermediate $Y =$ N 43°/4° and lengthening $X =$ N 161°/80° (Fig. 8b; Martino, Guereschi & Sfragulla, 2002) were determined following Marrett & Allmendinger (1990). These coincide with axes assigned to Event A (Kraemer *et al*. 1988) of probable Pliocene age, discussed by Martino *et al*. (1995).

At kilometre 827 of Provincial Route 28 (Fig. 8c) which crosses the Sierra de Pocho, anastomosing fault planes (0.20–6 m of damaged area) displaced mylonitic foliation ($S_m =$ N 330°/60° E with a stretching lineation $L_s =$ N 50°/54°) and intercalated amphibolite, the latter with epidote growth on the fault plane whose orientation is N 308°/9° NE with striations N 60°/8°. This fault is reversed, with tectonic transport direction to *c.* N 240° (Fig. 8d). This faulting coincides with Event B (Kraemer *et al*. 1988) of probable pre-Pliocene age, as discussed by Martino *et al*. (1995).

The brittle deformation suffered by the Los Túneles ductile shear zone developed cataclasis parallel to the main mylonitic foliation (plane C), producing a millimetre-thick brecciation, fracture cleavage and pseudotachylite generation. The latter forms concordant veins (< 7 cm thick), black to greenish, with discordant ramifications and a tree-like appearance. They contain clasts with mylonitic foliation and have mostly reverse kinematics (Martino, Guereschi & Sfragulla, 2002). Millimetre veins are also recognized, filled with calcite and chlorite, subperpendicular to the dominant foliation C.

Based on overlapping relationships as observed in the outcrops, the relative order of the recognized structures is: first the fracture cleavage, second the La Mermela fault zone, then the conjugated thrusts with concomitant development of kink-bands and drag folds in phyllites and mylonites and, finally, discordant veins (Martino, Guereschi & Sfragulla, 2002). Cataclasis and pseudotachylites parallel to the foliation C are associated with the conjugated thrusts. Whitmeyer (2008) argued that the minimum age of the Los Túneles pseudotachylites is *c.* 340–350 Ma, so that brittle deformation may have begun in the Carboniferous period. Reactivation of this structure also in a brittle regime, with development of gouge and brecciation, is probably linked to the Cenozoic deformation that produced the uplift of the sierras of Guasapampa and Pocho. The origin of the large asymmetrical synformal fold in sedimentary rocks (a drag fold?) could be a concomitant event.

3.b. Ciénaga del Coro – La Sierrita fault

The Ciénaga del Coro fault is a *c.* N 175°-striking, 40–50° E-dipping fault, curving eastwards in its southern section which uplifted the eponymous range over the Sierra de Guasapampa (Figs 4, 5). It is profusely covered with vegetation, in both the hangingwall and the footwall, making it difficult to access and study the materials involved. In the hangingwall, tonalitic rocks have a foliation N 330°/40–83° E and the fault trace is parallel to it, indicating a strong control on their nucleation. Mylonitized rocks and circulation of fluids that precipitated iron oxides and aragonite along the fault plane have been recognized (Lucero Michaut & Olsacher, 1981). This is a reverse fault with an impressive escarpment in its northern section which becomes lower and less steep towards its southern section, disappearing beneath the Tertiary volcanic rocks (Pocho Volcanic Complex, Fig. 4). Here the fault is probably combined at depth with the Ojo de Agua lineament (Caro Montero, Martino & Guereschi, 2015; see Section 4), which in turn combines with the La Sierrita fault forming a single structure with a sigmoidal trace on the map.

The La Sierrita fault uplifted a small NNW-striking block, slightly oblique to the Sierra Grande, with low-dip (30–40°) to the east. Internally the La Sierrita block (Fig. 2b) consists of mylonites and associated rocks from the Ambul–Mussi ductile shear zone. To the south, this fault ends at the Nono fault.

3.c. Cumbre de Gaspar – Nono fault

The traces of these two faults form opposed arcs on the map: the Cumbre de Gaspar fault is convex to the east and the Nono fault is convex to the west (Fig. 4). Together these are the only E-vergent faults (antithetical) in the Sierras de Córdoba, unlike all other faults (synthetic) described in this paper (Fig. 9a). The Cumbre de Gaspar minor block is raised by the eponymous fault to the east and flanked by the Sierra Grande fault (see following section) to the west, with a throw of *c.* 100 m on both sides. Near the river that runs along the Cumbre de Gaspar fault, gneisses have retrograded bands of red gouge, oriented N 10°/45° W, crossed by vertical extensional quartz veins. These fault zones clearly cut the dominant S_2 foliation in gneisses and migmatites, oriented here N 305°/38° E. The Cumbre de Gaspar fault is active at its northern end near Villa de Soto, with several earthquakes from 1997 to date with magnitudes of 2.5–4.5 on the Richter scale (see Instituto Nacional de Prevención Sísmica de Argentina, http://www.inpres.gov.ar/seismology/xultimos.php). It is noted here that the major morphogenetic faults in

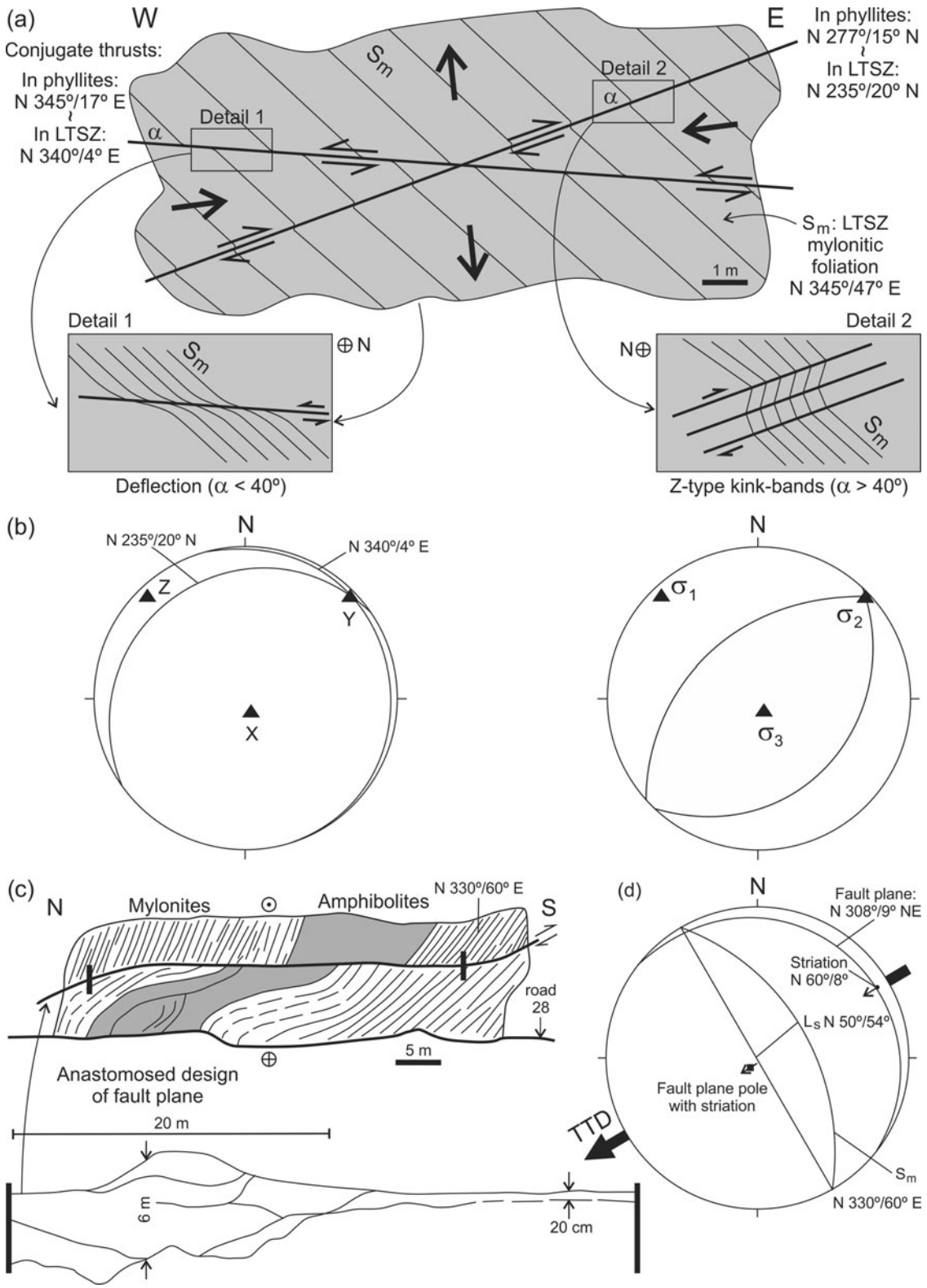

Figure 8. (a) Vertical west–east sketch showing minor conjugate thrust faults associated with the Sierra de Pocho fault, east of the La Mermela fault zone. These minor faults affected the fracture cleavage of the La Mermela phyllites and the mylonitic foliation (S_m) of the Los Túneles ductile shear zone (LTSZ) and are the result of brittle deformation superimposed on ductile deformation (drag folds and kink-bands, respectively), depending on the α angle between S_m and the faults. (b) Diagrams showing the kinematics and dynamics deduced from the conjugate thrusts (see text). (c) Anastomosed fault plane affecting mylonites and amphibolites. (d) Diagram showing structural relationships from (c). Both outcrops are located along Road 28 across the uplifted block of the Sierra de Pocho (see text for explanation). TTD – tectonic transport direction. See also Figure 7a.

Figure 9. (Colour online) (a) View to the south of the scarp of the Cumbre de Gaspar fault. This is the only W-dipping fault in the Sierras de Córdoba. Note that the footwall and the hangingwall slope gently to the west. This fault continues southwards to the Nono fault. (b) Oblique aerial view to the SE of the scarp of the Sierra de Comechingones fault. At the top in light colours is the gentle E-sloping Pampa de Achala horst-like elevation. Towards the footwall, the minor scarp of the Nono fault and the elbow of the Los Sauces river forming the reservoir of the La Viña dam are seen. (c) Detail from (b) showing the Pampa de Achala, with both sides limited by a series of reverse faults, E-dipping faults on the western flank and W-dipping faults on the eastern flank (see Fig. 4).

the Sierras de Córdoba have thin cataclastic zones that do not match, at first sight, with kilometre uplift of the respective blocks. Here, only decimetric fault zones are recognized as in the case of the Sierra de Pocho fault.

The Nono fault (Fig. 9b) was described by Kraemer *et al*. (1993) and Richardson *et al*. (2013) in the eastern margin of the Devonian Achalita pluton (below 'NF' in Fig. 4), which was raised 17 m above the Cenozoic fluvial sediments of the Nono valley. This is a thrust whose plane is oriented N 331°/41° W. The fault zone is *c.* 2 m thick with anastomosed geometry, and contains a breccia with intercalated clays. These rocks are striated and, along with other movement indicators, reveal the kinematic and temporal evolution of the fault. Sedimentary materials record two fault movements (late Pliocene and late Pleistocene) and two deformation events: (1) a more recent event, with shortening axis $Z = $ N 293°/3° and lengthening axis $X = $ N 43°/81° (recorded in breccia), and (2) another with shortening axes $X = $ N 20°/2° and lengthening axis $X = $ N 190°/74° (the older, of uncertain age).

The Nono fault was interpreted by Kraemer *et al*. (1993) as a backthrust of the Sierra de Pocho fault (Fig. 4). This backthrust is interpreted here as continuing to the north in the Cumbre de Gaspar fault. Together they form an uplifted block with rocks belonging to the middle crust of the San Carlos massif (*c.* 1000 km^2 of anatectic rocks), indicating that part of the uplift of the entire massif was Tertiary which, in combination with the Sierra de Pocho fault (throw *c.* 1000 m), forms a regional pop-up structure (P on the map in Fig. 4).

3.d. Sierra Grande – Sierra de Comechingones fault

This major fault uplifted the central range of the Sierras de Córdoba (Fig. 4), the Sierra Grande, located between the Sierra Chica (east) and the Sierra de Pocho (west), and its southern continuation in the Sierra de Comechingones (Fig. 9b). It is a N-striking, straight trace, high-angle (45–55° E) reverse fault, extending more than 250 km at approximately longitude 65° W.

In the central section, coinciding with the southern portion of the Achala batholith, it is divided into a series of parallel faults forming tectonic steps. The southern portion of the Achala batholith can therefore be interpreted as a horst-like elevation, limited on both flanks by a series of reverse faults E-dipping in the western flank and W-dipping in the eastern flank. The result is a high plain called Pampa de Achala, sloping slightly to the east (Fig. 9c) and probably of Palaeozoic origin (Schmieder, 1921; Jordan *et al*. 1989). The vertical throw caused by the faulting in the western flanks of the Sierra Grande and Sierra de Comechingones is 1800–2000 m, while on the eastern slope of these ranges it is *c.* 1500 m. To the north, the Sierra Grande fault decreases in vertical throw and almost disappears. In the central area of the map (Fig. 4) and in the geological section A–A' (Fig. 5), the horst-like structure is labelled H and the tectonic steps with numbers.

The morphotectonic steps raised the highest peaks in the granitic rocks of the Achala batholith (Cumbre de Achala) in the Sierra Grande. To the south in the Sierra de Comechingones the highest peaks were produced in high-grade metamorphic rocks, including the Cerro Champaquí (2884 m a.s.l.), the highest elevation in the Sierras de Córdoba. Red cataclastic zones derived from granite, 300–500 m thick, are identified in a few of these faults, sometimes cemented by ferruginous silica solutions and calcareous material. To the south, the Sierra de Comechingones fault also decreases in vertical throw and is divided into three minor reverse faults, forming small ranges of oblique arrangement which together form a horsetail end (Fig. 4).

In the Sierra de Comechingones fault, the main trace is located at the intersection of the escarpment with the piedmont covered by modern sediments; descriptions of outcrops are therefore not available to date. Inside the piedmont however, low scarps parallel to the main scarp are recognized and defined as piedmont forelands (Bull, 2007). These geomorphological features are an expression of Quaternary fault activity; one of them, the El Molino fault near Merlo town (Fig. 4), was dated by optically stimulated luminescence (OSL) techniques as 7.1 ± 0.4 ka and 350 ± 40 ka BP (Costa *et al.* 2014).

The Sierra de Comechingones fault is a structure that could have a significant Palaeozoic vertical displacement of several kilometres based on magnetic data at its southern end (Chernicoff & Ramos, 2003). Bense *et al*. (2011) proposed early Carboniferous fault activity followed by Permian–Triassic and Jurassic events, based on K–Ar fault gouge data. Considering this together with the neotectonic activity the structure seems to have been active from ancient times, and the current high relief was probably not entirely caused by the effect of the Andean flat-slab.

3.e. Sierra de Cunuputo fault

This is a minor fault compared with the other major faults, but raised the important eponymous range in the northern part of the Sierra Grande (Fig. 2a). In its northern third it shows a Y-shape on the map with a branch called the San Marcos fault, which raised a small block known as the Sierra Baja de San Marcos. The Sierra de Cunuputo fault has experienced neotectonic activity in two stages during late Holocene time, evidenced by changes in the drainage network, terraces and lacustrine deposits (Massabie, 1982; Massabie *et al*. 2003; Costa *et al*. 2014).

3.f. Sierra Chica fault

This is one of the most important and best-studied faults in the Sierras de Córdoba (Fig. 4). Its fault scarp extends for more than 200 km from Capilla del Monte, in the northern Punilla Valley to near the Los Cóndores lineament. From here the fault branches into a series of lineaments, among which the Elena lineament, with a curved trace, which is the western margin of the Sierra

de Las Peñas (Martino, Guereschi & Carignano, 2012). Its highest elevation is Cerro Uritorco, east of Capilla del Monte (1950 m a.s.l., Fig. 2a).

The trace of the Sierra Chica fault consists of straight and curved segments. The straight segments are high-dipping faults (50–60° E) that form the boundary of Cretaceous deposits, and are therefore interpreted as reactivated Cretaceous normal faults. In contrast, the curved segments are low-dipping reverse faults (≈ 30° E), not associated with any particular deposit, and are interpreted as new Tertiary faults (Schmidt *et al.* 1995; Painceyra, 1998); they were defined as basement thrusts by Martino *et al.* (1995).

The hangingwall of the Sierra Chica fault is composed of the metamorphic basement, mainly gneisses and migmatites more or less altered, for example in the Santa Rosa area (Figs 10c, 11) where the metamorphic basement is strongly altered and brecciated, losing the primary structure of the rocks (metamorphic foliation S_2).

Throughout its sinuous trace, the Sierra Chica fault thrust rocks of different lithologies and depositional ages. In the area of La Cumbre town it affects Cretaceous conglomerates; in the Cosquín area, it thrusts Tertiary strata of the Punilla Valley (Fig. 11a) partially over Pleistocene fanglomerates in the Villa Carlos Paz area (Fig. 10b) and over Quaternary conglomerates (Figs 10c, 11) in the Santa Rosa area (Castellanos, 1944, 1951; Gross, 1948; Schlagintweit, 1954; Lencinas & Timonieri, 1968; Massabie 1976, 1987; Gordillo & Lencinas, 1979; Kraemer *et al.* 1988; Massabie & Szlafstein, 1991; Kraemer & Martino, 1993; Martino *et al.* 1995; Schmidt *et al.* 1995). In the Potrero de Garay area (Fig. 10d), the Sierra Chica fault rides over recent soils (Costa *et al.* 2014). The overthrust relationship southwards on younger sedimentary rocks and then soils indicates diachronism in fault propagation in this direction.

In the Cosquín area (Fig. 4) in particular there is a sequence of synorogenic Tertiary sedimentary rocks (Fig. 11a) with two formations in relative structural concordance, separated by a calcrete horizon (Linares, Timonieri & Pascual, 1960; Lencinas & Timonieri, 1968). The lower sequence of late Eocene – early Oligocene age (Cosquín Formation, age based on mammals fossils) is composed of clasts of granitic material from the Achala batholith (located to the west), indicating a provenance from Sierra Grande which was rising west along its eponymous fault. The upper sequence of probable late Miocene – Pliocene age (Casagrande Formation) is paraconformable and composed of clastic material from the metamorphic basement typical of Sierra Chica (gneisses, pegmatites, granodiorite and tonalite). This synorogenic sequence evidences the uplift of the Sierra Grande block before Sierra Chica, indicating the relative timing of activity of the eponymous faults. In Figure 11a, these sedimentary sequences are shown imbricated by the latest activity of the Sierra Chica fault. The imbrications of the sedimentary sequences allow the steepening of the main fault plane (thrust rotation) to be deduced. The main fault started as a basement thrust and, as the deformation progressed, the synorogenic sedimentary sequences became involved by successive underthrusts propagating towards the west. Consequently, a stacking of the underthrusting wedge, with progressive back-rotation of the succesive faults, was produced. Older faults therefore have an angle progressively higher than the younger faults. This mechanism is illustrated in Figure 11a.

At more regional scale, Sierra Chica intercepts drainage from Sierra Grande by deviating or maintaining its original course and pattern (antecedent rivers). This also implies that the uplift of Sierra Chica postdated the uplift of Sierra Grande (Gordillo & Lencinas, 1979).

Along the Sierra Chica fault zone, there is variable development of brittle deformation along with chemical changes in the rocks. At the latitude of Quebrada Honda (Fig. 12a), cataclasites associated with the Sierra Chica fault zone are recognized: 2–4 m of microbreccias with red and green fault gouge, followed by 10–30 m of breccias. To the east, the fault affected the regional metamorphic rocks in a belt 200–400 m thick, reworking the foliation of the gneisses and retrograding biotite to chlorite ± muscovite. In the Villa Carlos Paz area rocks related to the fault zone are phyllonitic, intensely chloritized and with secondary muscovite, with a strong orientation that defines a lineation N 70°/45° on the foliation plane. Acid igneous material is intercalated in three patterns: (1) deformed lenses, parallel to the main foliation plane; (2) asymmetrical folds; and (3) normally displaced pegmatite.

In a few locations, the outcrops allow kinematic analysis of the fault plane. At the latitude of Villa Carlos Paz (Fig. 12a, c) south of Quebrada Honda, kinematic and dynamic analysis of minor faults associated with the main faults revealed two mutually orthogonal compressive events. For Event A, the shortening axis is Z = N 106°/11° and for Event B it is Z = N 15°/3° (Painceyra, 1998). Further north in the Cosquín area (Figs 11a, 12b), the kinematic analysis of minor faults in the hangingwall shows two populations of faults: a well-developed reverse-type with shortening axis Z = E to SSE (Fig. 12b); and another strike-slip component poorly represented with shortening axis Z = NE, similar to results in other areas of the Sierras de Córdoba. A deformation event post-dating the piedmont deposits is clearly recognized (Fig. 11a). However, the sedimentary record supports the existence of at least two previous reactivation events, without a precise time location, revealing the complex history of this structure in which shortening is produced by reverse faults (Kraemer & Martino, 1993).

Particularly interesting due to its proximity to the Río Tercero dam and nuclear power plant is the description of the Sierra Chica fault near the Santa Rosa. Here the metamorphic basement, formed mainly of gneisses and migmatites, is thrust over Quaternary sediments along a gentle E-dipping fault plane (Fig. 11b). This structure, known locally as the Santa Rosa fault, was first

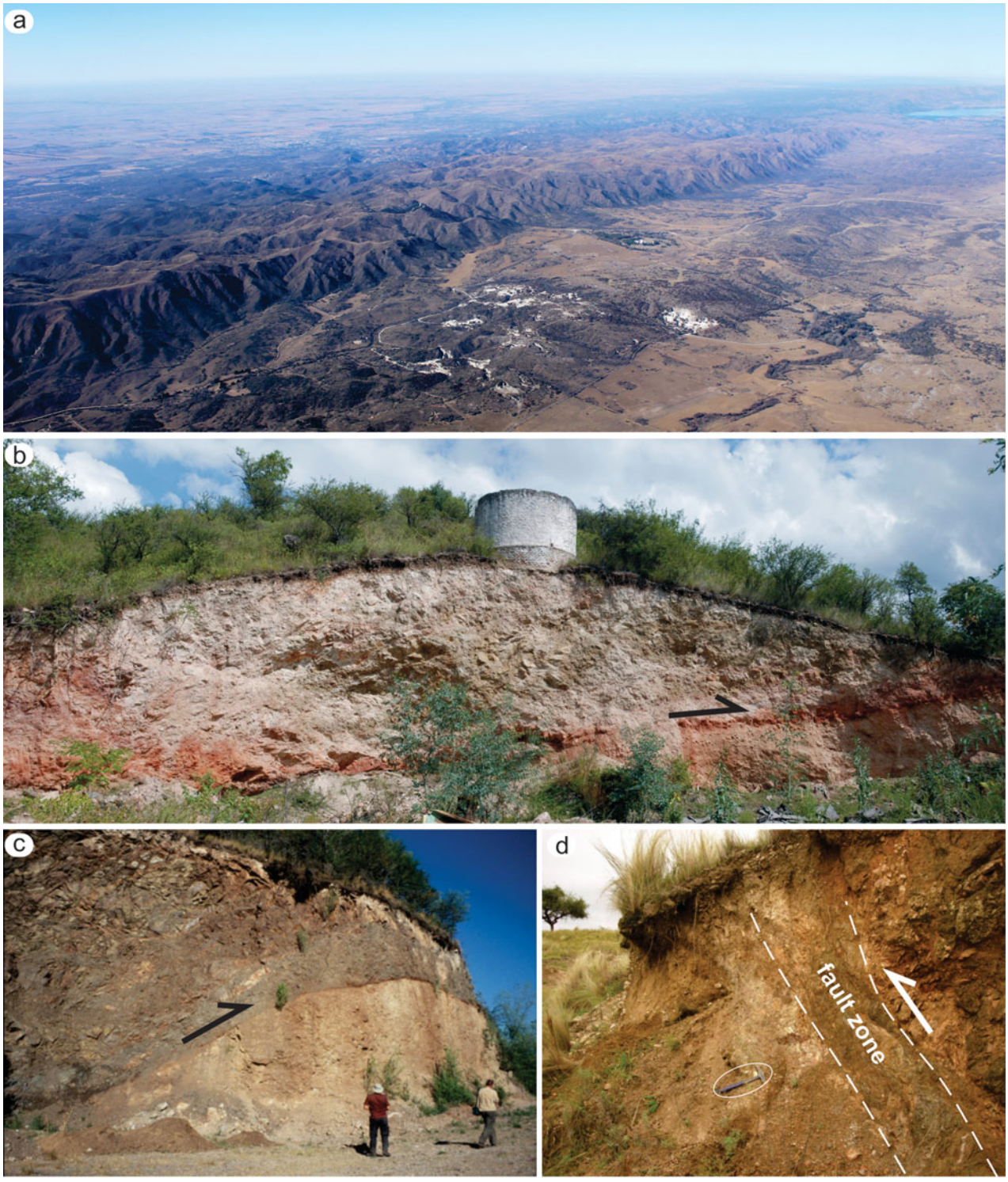

Figure 10. (Colour online) (a) Oblique aerial photograph of the scarp of the Sierra Chica fault at the latitude of the city of Alta Gracia; view towards the SE. Note the curvature of the fault trace. Main outcrops of the Sierra Chica fault: (b) El Tanque quarry, Villa Carlos Paz area, east–west profile; (c) Santa Rosa area, east–west profile; and (d) Potrero de Garay area, west–east profile. In (b) and (c), the metamorphic basement rides over Cenozoic sedimentary rocks. In (d), the fault affected recent soils (hammer scale in the ellipse). See text for details.

described by Massabie (1987), whereas Kraemer *et al*. (1988) made the first kinematic and dynamic study. The local strike of the fault is N 340°, E-dipping between 30° and 40° (Figs 2, 10c). The hangingwall consists of highly altered, brecciated, dark-green quartz-feldspar gneisses, fractured such that the rock is divided into irregular polyhedrons having lost its primary structure (metamorphic foliation S_2). The footwall is formed of pale yellow sedimentary rocks with coarse stratification, composed of clasts of variable size (10–120 cm diameter) within a conglomeratic sandy matrix, interpreted as piedmont cenoglomerates produced by debris

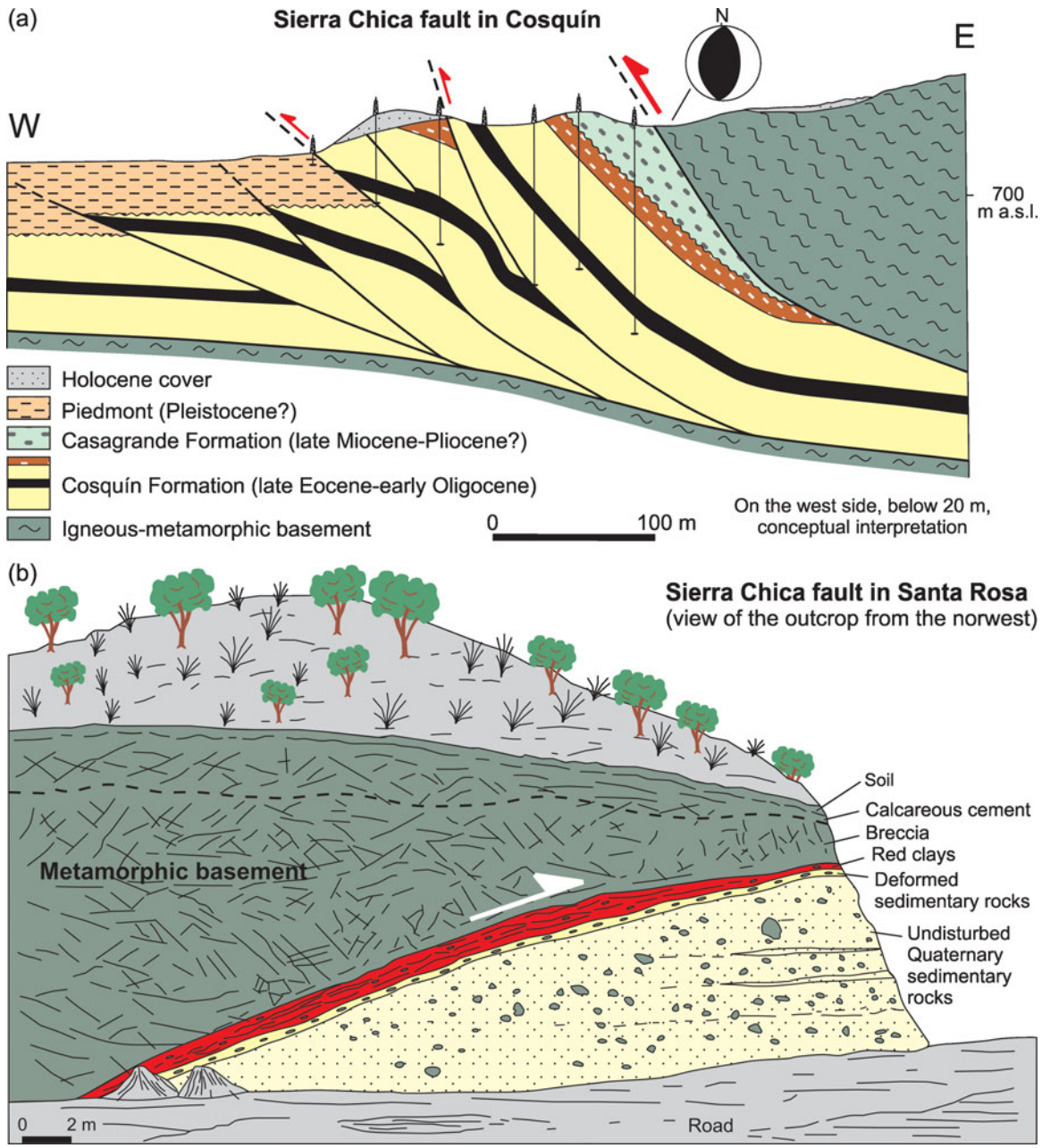

Figure 11. (Colour online) Detailed geological sections of the Sierra Chica fault. (a) In the Cosquín area, the igneous–metamorphic basement is thrust over Tertiary sedimentary sequences, imbricated by the latest activity of the Sierra Chica fault. High angles in the fault planes are interpreted as the result of translation and progressive back-rotation of the basement as the imbrication of the sedimentary wedge occurred below, implying the steepening of the main fault plane (bold arrow; modified from Kraemer & Martino, 1993). (b) In the Santa Rosa area the metamorphic basement, formed mainly by gneisses and migmatites, is thrust over Quaternary sediments along a gentle E-dipping fault plane (modified from Kraemer *et al.* 1988). See text for details and Figure 12 for location and kinematic analysis.

flows coming from the east. A red clay zone is identified in the fault plane with a thickness varying over the range 10–80 cm, which shows cataclastic foliation with striations and push marks clearly revealing the relative motion of the blocks. Upwards above the fault plane, the basement rocks are intensely fractured and contain minor faults and kinematic indicators. The sedimentary rocks below the fault plane are weakly deformed within a layer no thicker than 20 cm, with carbonate cement in which clasts of metamorphic rocks were reorientated parallel to the fault plane (Fig. 11b). The analysis of minor faults allows recognition of two deformation events (Fig. 12d): Event A, with shortening axis Z NW (N 288°) and subvertical lengthening axis X; and Event B, with shortening axis Z NE (N 53°) and near-horizontal lengthening axis X.

The minimum age of deformation on the Sierra Chica fault depends on the age assigned to the sedimentary sequences overthrust by the basement. Based on the correlation of similar rocks in different areas in the Sierras de Córdoba, these are probably middle–late Pleistocene in age. Event A is clearly recognized

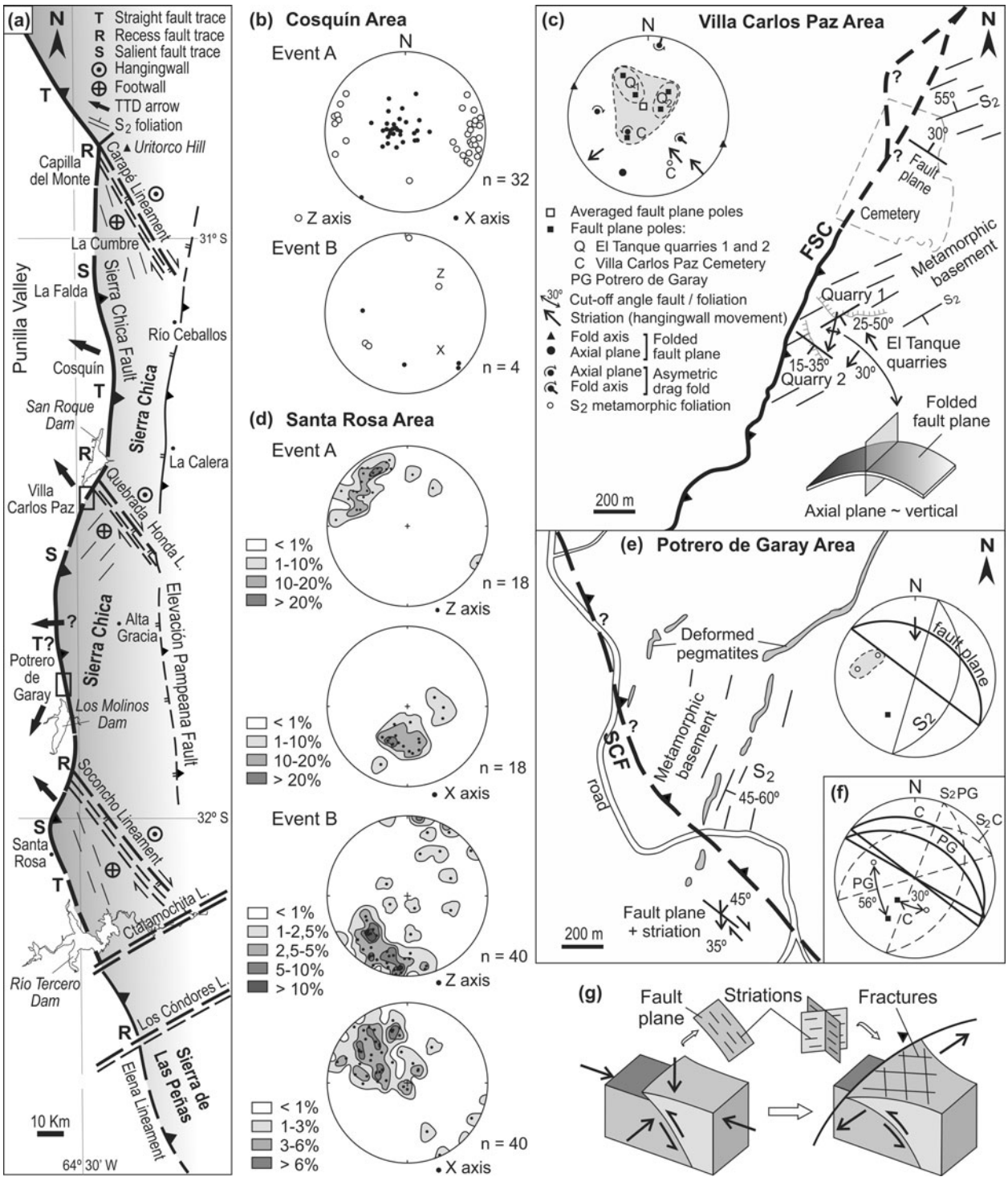

Figure 12. (a) Interpretive map of the brittle structure of the Sierra Chica (modified from Martino, Guereschi & Carignano, 2012) showing different areas of outcrops of the Sierra Chica fault (SCF). Arrows TTD – tectonic transport direction. (b) Shortening and lengthening directions deduced for deformation events A and B in the Cosquín area (Kraemer & Martino, 1993). (c) Detailed map of the structure and structural data (lower-hemisphere Schmidt net) for the Villa Carlos Paz area. (d) Directions of shortening and lengthening deduced for deformation events A (*Z* axis NW shortening direction = N 288° and *X* axis subvertical lengthening direction) and B (*Z* axis NE shortening direction = 53° N and *X* axis close to horizontal lengthening direction) in the Santa Rosa area (Kraemer *et al.* 1988). (e) Detailed map of the structure and structural diagram data in the Potrero de Garay area. (f) Cross-cutting relationships between the dominant metamorphic foliation S_2 and fault planes in the areas of Villa Carlos Paz and Potrero de Garay. (g) Scheme showing the expanding front of the basement thrust sheet from the Sierra Chica fault, with minor associated fracturing (not marked on the map) for example between the Quebrada Honda and Soconcho lineaments, which behaved as lateral ramps.

in clay levels along the fault plane as the last movement of the structure, so its age would be post-middle Pleistocene (late Pleistocene?). Event B is recorded in the thrust basement relatively far from the fault plane and is considered as a previous event of uncertain age. By correlation with faults in other studied areas, a late Pliocene (?) age is assumed.

3.g. Elevación Pampeana fault

As for the other morphogenetic fractures in the Sierras Pampeanas, this is a N-striking, E-dipping reverse fault (Figs 4, 5) with a short range from Río Ceballos to the Soconcho lineament (Bodenbender, 1929; Gordillo & Lencinas, 1979). This fault is the western limit of the Cretaceous red strata on the eastern flank of Sierra Chica. To the east, the boundary of these sedimentary rocks is erosive or they underlie recent deposits of the Chaco-Pampean plain. The fault is therefore also interpreted as a normal fault inverted during the Tertiary Andean orogeny. It is the final thrust fault of that age that limits the Sierras de Córdoba with the Chaco-Pampean plain, defining the landscape morphology. Although the age of the last movement of the Elevación Pampeana fault is unknown, it is estimated that its formation is more recent than that of the Sierra Chica fault.

The small Elevación Pampeana range is composed of biotite gneisses, amphibolites and calcic marbles, intruded by aplitic and pegmatitic acid igneous rocks. In the La Calera area, a zone of crushed gneisses (*c.* 50 m thick) grades to finer materials until it becomes a brown fault gouge with rounded and polished clasts of different size. Rotated blocks of marble are observed in some quarries, intensely brecciated and with widespread friction marks.

The predominant style of the Sierras Pampeanas, with a steep western scarp and gentle eastern slope, is also recognized. Altitude increases northwards from 590 m a.s.l. (Alta Gracia) to 700 m a.s.l. (Cerro Largo, La Calera, Fig. 4). The fault movement produced the ESE-tilting of the hangingwall at an angle of 10–12° near the fault, decreasing to 4–5° towards the city of Córdoba. The regional tilting of the basement determined the ESE topographic slope that controls the flow of the main rivers at this latitude (Fig. 6).

4. Oblique lineaments

Gross (1948) drew attention to large linear features oblique in the Sierras de Córdoba, >100 km long in some cases and of maximum width 100 m, suggesting they had a profuse pattern of internal fracturing. However, in most cases there is no visible deformation other than the linear geomorphological feature. Petrographically, retrograde biotite replaced by muscovite and chlorite is commonly observed. In several cases, ductile shear zones producing mylonites are linked to these lineaments (Martino, 2003).

A set of lineaments 2.5–5 km apart occurs in the northwestern sector of the Achala batholith (Fig. 4; Martino, Toledo & Guereschi, 2012): Candelaria, Corral del Carnero, Rincón Grande, Guasta and Retamito (Fig. 13). These lineaments are NNW-striking, almost vertical planes; the traces are straight to slightly bent and a few of them have minor Y-shaped branches (e.g. the Candelaria lineament). They define deep V-shaped valleys and segment the Achala batholith and the northwestern metamorphic host rocks in a series of elongate NNW blocks (Fig. 2). Paleocene olivine nephelinite dykes occur along the Guasta lineament (Gordillo, Linares & Daziano, 1983).

One that stands out is the Retamito lineament (Fig. 4) that cuts across the San Carlos massif, the Achala batholith and its southeastern metamorphic host rocks. In the central area, it uplifted the granite block of Cerro Los Gigantes (2400 m a.s.l., Fig. 13). In combination with reverse faults, this structure generated significant metallotects (e.g. uranium; Blasón, 1999). Another important structure is the seismically active Ojo de Agua lineament (Fig. 4); to the SE it continues in the Soconcho lineament, forming a single structure at regional scale with a total length of *c.* 120 km. This structure has a branch to the Retamito lineament. On the surface, zones of mylonitic rocks parallel to the Ojo de Agua lineament, currently under study, have been recognized. Brittle faulting controlled by these zones of mylonites and by the lineament is also produced. Based on seismic activity, Caro Montero, Martino & Guereschi (2015) defined an almost vertical planar structure which coincides with the Ojo de Agua lineament (Fig. 14*a*, *b*). Both the La Sierrita fault and the Ciénaga del Coro fault merge into this lineament forming a single structure, whose merging area is the most seismically active in the region. Analysing several perpendicular sections, the depth of this structure reaches *c.* 84 km (Fig. 14*b*, *c*) with sinistral transpressive kinematics (see Section 7).

Another notable lineament is the La Higuera–Dos Pozos lineament (Fig. 4) in which a Tertiary reverse fault was nucleated, with the hangingwall towards the NE and the footwall towards the SW. The footwall is coincident with the homonymous ductile shear zone developing mylonites. Auriferous quartz veins occur along the lineament.

With the same features of the La Higuera–Dos Pozos lineament, but with the ductile shear zone in the hangingwall, is the Pachango lineament (Fig. 4). This reworked the homonymous ductile shear zone and juxtaposed high-grade rocks and the Los Túneles ductile shear zone with medium-grade rocks cropping out to the south in Sierra de Altautina (Fig. 7a). In the last range, several lineaments are recognized (e.g. La Cocha, La Viña). In the Nono Valley, exceptional illite deposits (>1 km long) produced by hydrothermal alteration of schists have been recognized (Bertolino & Murray, 1992). A vertical throw of 15–30 m is associated with this oblique faulting (Olsacher, 1972).

As with the above-described lineaments, in the Sierra Chica oblique lineaments are associated with ductile and brittle shear zones with complex deformational

Figure 13. (Colour online) View to the SE of Quebrada Retamito, where the eponymous lineament raised the granite block of Cerro Los Gigantes (right in the picture silhouetted against the horizon). Cataclastic rocks occur along this lineament.

histories. From north to south, they are the Deán Funes, Carapé and Soconcho lineaments (Figs 4, 12), among others.

Using the receiver function method, Perarnau *et al*. (2012) and Richardson *et al*. (2013) obtained data from 16 seismographs throughout the Eastern Sierras Pampeanas. Information on discontinuities in the crust and the upper mantle at the latitude of the Sierras de Córdoba revealed NE shifting and relative sinking (*c*. 3 km, Figs 4, 5) of the Mohorovicic discontinuity, coincident with the oblique lineaments recognized in Sierra Chica and its prolongation to the NE.

One of the most important is the Deán Funes lineament (Fig. 4), which extends for more than 200 km with a width of the order of kilometres. This lineament is coincident with one of the most marked structural trends in the Cretaceous tectonics of Argentina and extends towards the Atlantic margin in the Salado basin (Fig. 1). The current sinistral movement with a normal component (transtensive or oblique divergent shear) is recognized to a depth of more than 40 km, where it displaces the Mohorovicic discontinuity (Gilbert *et al*. 2010) by 3 km (see Section 7).

The Carapé and Soconcho lineaments (Fig. 4) are linked to Cretaceous tectonics as limits of the pull-apart extensional basins of the sierras of Pajarillo, Copacabana and Masa and Sierra de Los Cóndores, respectively (Martino *et al*. 2014). The Soconcho lineament can be continued to the NW, integrating with the Ojo de Agua lineaments with a branch to the Retamito lineament as described earlier in this section. These lineaments form a segmented crustal discontinuity on the map, with a more or less straight trace indicating high-dipping. In some places, the main trace can be resolved in several parallel or overlapping traces such as between the Ojo de Agua and Soconcho lineaments (Fig. 4).

Both Carapé and Soconcho lineaments also show at depth a vertical shifting of the Mohorovicic discontinuity (Perarnau *et al*. 2012; Richardson *et al*. 2013) similar to the Deán Funes lineament (see Section 7).

In general it is noted that the oblique lineaments are associated with brittle deformation, in some cases Tertiary age as in the La Higuera–Dos Pozos and Pachango lineaments. The Ojo de Agua lineament has also current seismic activity. Another important point is that several lineaments are very deep (Ojo de Agua, Deán Funes, Carapé, Soconcho), and some of them shift the Mohorovicic discontinuity. In other cases brittle deformation would be older, associated with Cretaceous tectonics as in the Soconcho and Carapé lineaments. This brittle deformation is associated with Palaeozoic ductile shear zones both in the hangingwall and in the footwall of the current faults.

One possible interpretation is that these lineaments, or parts of them, are probably ancient features inherited from pan-Gondwanan structures (Daly, 1988; Tankard *et al*. 1995), which worked in a protracted time period,

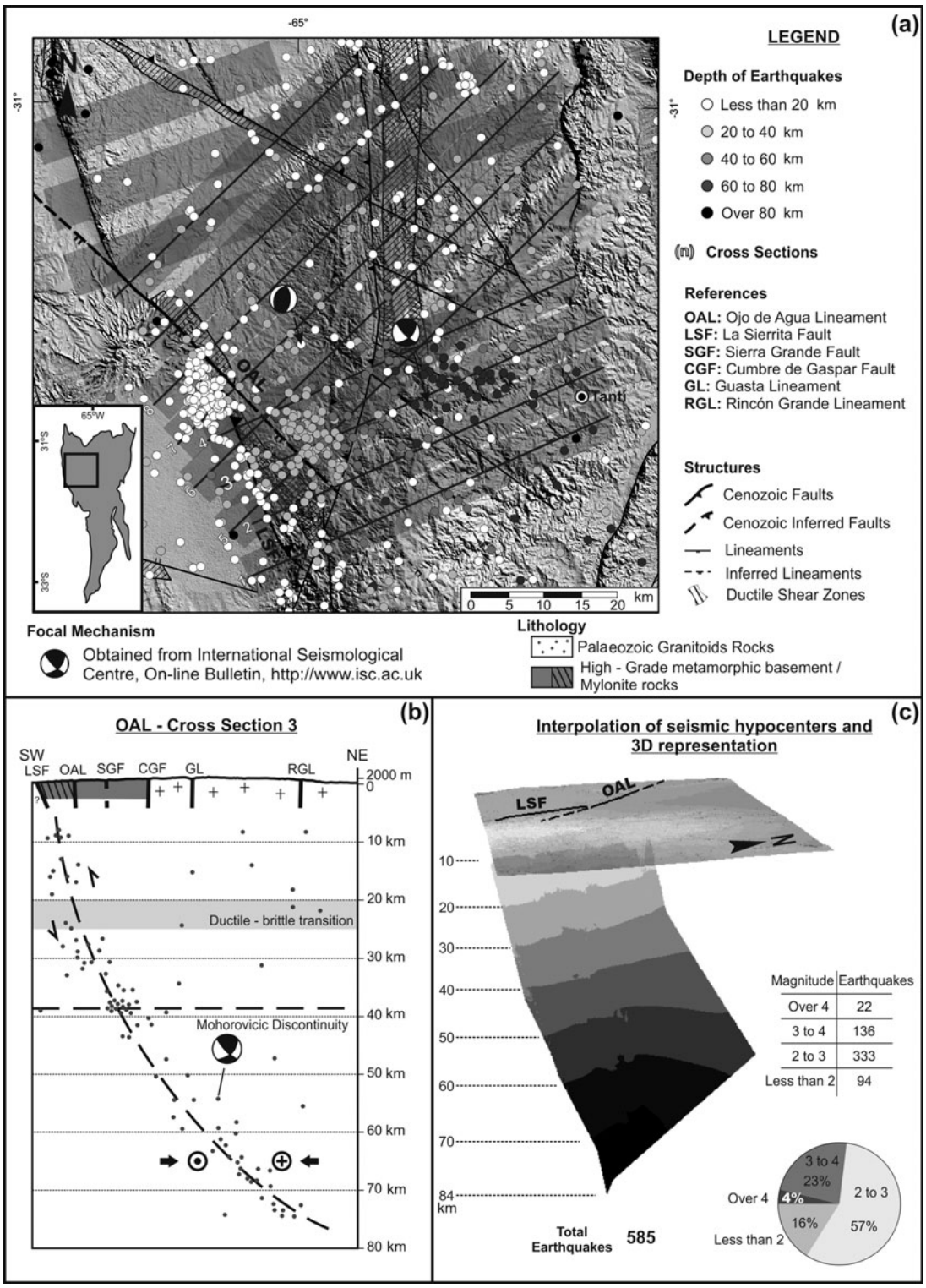

Figure 14. Study of the epicentre and hypocentre locations of earthquakes in a northwestern sector of the Sierras de Córdoba (Caro Montero, Martino & Guereschi, 2015). (a) Digital elevation model (DEM) on which the earthquakes recorded in the area, from May 1923 to August 2015, are classified by depth. Total number of earthquakes: 585 (115 at >40 km depth and 470 at <40 km depth). Database from Instituto Nacional de Prevención Sísmica in Argentina, United States Geological Survey and T. Richardson (unpub. PhD thesis, Purdue University, 2011). Two focal mechanisms obtained from the International Seismological Center. (b) Cross Section 3 perpendicular to the Ojo de Agua lineament. Equal vertical and horizontal scales. (c) 3D representation of the Ojo de Agua lineament by interpolating earthquakes in 10 sections, showing the trend observable in Cross Section 3. Circle chart and table show the magnitudes (M_b) of the earthquakes that have been included in this study.

controlling the Palaeozoic, Mesozoic and Cenozoic deformation.

5. Fault-related folds

Tertiary folds are recognized in Eocene sedimentary rocks (Linares, Timonieri & Pascual, 1960) in the footwall of the Sierra Chica fault in the Punilla valley, near the town of Cosquín (Fig. 12a). These rocks have a homoclinal arrangement but in same places are folded, probably in relation to the basement uplift. Hectometre-sized open folds, with E-dipping axial planes and subhorizontal axes dipping both north and south (Lucero Michaut, 1976) can be assigned to drape folds.

At the latitude of Villa Carlos Paz (Fig. 12a), W-vergent, asymmetric drag folds and upwardly open gentle folds, both metre-scale, are recognized in cataclastized gneisses in the hangingwall of the Sierra Chica fault (oriented here N 40°/30° E).

Other drag folds are clearly visible in the contact of the Los Túneles ductile shear zone with the La Mermela phyllites, reflecting the effect of the Sierra de Pocho fault. Chevron folds, with subhorizontal axes and axial planes oriented N 10°/42° W, affect the dominant foliation in phyllites, which outside the contact area is oriented N 0°/40° E (Fig. 7c).

A W-overturned open syncline, hundreds of metres wide and long, with an E-dipping axial plane and subhorizontal axis, is recognized in the piedmont of the Sierra de Pocho near Chancaní (Fig. 7a). This fold is formed by drag on the footwall of the Sierra de Pocho fault in subhorizontal Carboniferous sedimentary rocks (sandstones of the Chancaní Formation, Fig. 7b). This is one of the largest folds recognized due to Tertiary deformation in the Sierras de Córdoba.

6. Estimation of uplift, maximum displacement and tectonic transport direction of main thrusts

Elliott (1976) published a figure showing the maximum displacement in thrust faults as a function of length along strike. The relationship between the maximum displacement D and fault length L is usually considered to be of the form $D = \gamma\ L\ C$, where γ is the proportionality constant and C has a value between 1 and 2 (Cowie, 1998; Groshong, 2008). The precise relationship seems to depend on many factors, including mechanical stratigraphy and nature of the interactions between overlapping faults. For a practical estimate of this relationship in a map interpretation, we assumed $C = 1$, leading to $\gamma = D/L$. Ratios of 1:8 to 1:33 are common, regardless of location, size or type of fault.

Displacement on the main faults of the Sierras de Córdoba has not yet been measured but it is possible to apply the bow-and-arrow rule of Elliott (1976) to some typical thrusts, measuring the length of the exposed faults on the map, in order to estimate the maximum displacement and the tectonic transport direction. We have selected only the main low-dipping (thrusts) and curved trace faults that we interpret as new reverse faults produced by Cenozoic deformation.

The results are displayed in Figure 6 and the inset table, indicating that the maximum fault displacement decreases eastwards, ranging between 8.8 km and 3.2 km. The displacement/length ratio varies between 1:12 and 1:6, with an average of 1:8.4 ($\gamma = 0.13$). The deduced tectonic transport direction (TTD) is relatively constant towards the west (*c.* N 260–270°).

In the Sierras de Córdoba, block uplift over the surrounding valleys and plains (*c.* 300–400 m a.s.l.) and the highest elevations in each range decrease from west to east: Sierra de Pocho (Cerro Agua de la Cumbre, 1577 m a.s.l.); Sierras of Comechingones–Grande (Cerro Champaquí, 2884 m a.s.l.); Sierra Chica (Cerro Uritorco, 1950 m a.s.l.) and Elevación Pampeana (Cerro Largo, La Calera, 700 m a.s.l.).

In addition, the synorogenic deposits in the piedmont of the Sierra Chica fault (Fig. 11a) clearly indicate an uplift of Sierra Grande prior to that of Sierra Chica uplift, demonstrating the relative timing of activity of the eponymous faults.

In summary, Cenozoic block uplift, the maximum displacement of the fault thrusts and the age of faulting all decrease from west to east (sequentially faulted hangingwall). It follows that faulting propagated from west to east. In this context, we suggest that the Río de la Plata craton, which lies at depth beneath the Chaco-Pampean plain, acted as a buttress to Andean compression in the Eastern Sierras Pampeanas (backwards propagation faulting).

7. Faulting depth

How faults extend at depth is a major problem. González Bonorino (1950) proposed that the Sierras Pampeanas faults that produced block uplift would become horizontal with depth, brittle deformation at shallow depths being a result of compression. Downwards plastic deformation absorbs brittle deformation and would result in upper crust displacement over the lower crust along roughly horizontal planes. Geophysical data (Introcaso, Lion & Ramos, 1987; Alvarado *et al*. 2005; Alvarado, Machuca & Beck, 2005, Perarnau *et al*. 2012; Richardson *et al.* 2013) confirm the correctness of the intuition and geological and mechanical knowledge of González Bonorino (1950). Perarnau *et al*. (2012) and Richardson *et al.* (2013) carried out detailed studies showing the intracrustal structure of the Eastern Sierras Pampeanas, including estimates of crustal thickness and its variation as well as the location and displacement of Mohorovicic discontinuity.

The geological section A–A' (Fig. 5) cuts across the middle of the Sierras de Córdoba at about 31° 50′ S, crossing the main N-striking faults that uplifted the sierras of Pocho, Grande, Chica and Elevación Pampeana and the NW lineaments that obliquely intersect the section. Favetto *et al*. (2008) performed a magnetotelluric survey over 450 km through the Sierras de Córdoba, obtaining data to a depth of 200 km. Subsequently,

Orozco *et al*. (2013) complemented this study with another section that included the Precordillera, the Sierras Pampeanas and the Chaco-Pampean plain. In both studies, the boundary between the Río de la Plata craton and the Pampia terrane is located to the east of Sierra Chica, as a subvertical discontinuity marked by the difference between the resistivities of rocks in the two domains.

The Río de la Plata craton of Palaeoproterozoic age (2200–1700 Ma, Rapela *et al*. 2007), covered by several thousand metres of sediments from the Chaco-Pampean plain, acted as a rigid wall which was unaffected by Andean orogenic compression. Therefore, we propose that the suture between the Pampia terrane and Río de la Plata craton is the origin of the different take-off levels of the most important thrusts. Although this craton apparently reaches depths far greater than those established for the Mohorovicic discontinuity by Perarnau *et al*. (2012), we assume an average crustal thickness of 40 km or less as defined by satellite gravimetry and crustal thickness modelling for the continent (Assumpção, Feng & Julià, 2013; Van der Meijde, Julià & Assumpção, 2013). The depth of brittle–ductile transition zone is between 20 and 25 km, according to data obtained by Perarnau *et al*. (2012), with the depth of the Mohorovicic discontinuity between 38 and 40 km. These estimates are consistent with global geophysical studies for the South American continent (Assumpção, Feng & Julià, 2013; Van der Meijde, Julià & Assumpção, 2013) and, more locally, for the Andes (Gilbert, Beck & Zandt, 2006; Heit *et al*. 2008; Perarnau, Alvarado & Saez, 2010). The take-off level of these thrusts is defined as at 23 km, with slight variations caused by a major oblique lineament (Soconcho). These very pervasive lineaments cause an almost vertical shifting of the Mohorovicic discontinuity by 2.5–3 km (see fig. 4b in Perarnau *et al*. 2012).

As for section A–A', section B–B' (Fig. 5) is transverse to the Sierras de Córdoba in the northern part (at *c*. 31° 20′ S). As in the previous section, we have interpreted the boundary between Pampia Terrane and Río de la Plata craton as the place where the take-off levels of the main thrusts were generated. The zone of brittle–ductile transition is established at the same depth as in section A–A' (20–25 km), as is that of the Mohorovicic discontinuity (40 km or less), according to data obtained by Perarnau *et al*. (2012). To the east, near the end of the section, an almost vertical displacement of this discontinuity by nearly 3 km is caused by another important lineament affecting the Sierras de Córdoba (Carapé, see fig. 5b in Perarnau *et al*. 2012).

Crustal thickness ranges from 38 km in the west to 35 km in the east, and there are small variations in morphology of the Mohorovicic discontinuity (Perarnau *et al*. 2012) showing displacements of *c*. 3 km near the Soconcho, Carapé and Deán Funes lineaments. Two planar intracrustal structures are detected throughout the Sierras de Córdoba (remnants of hidden Cambrian crust?), displaced at depth by the main faults described in this paper. These faults have a listric, concave-up geometry, and are rooted between 22 km in the east and 27 km in the west over a ductile aseismic area *c*. 8–10 km above the Mohorovicic discontinuity (Perarnau *et al*. 2012). Geological sections (Figs 4, 5) were performed, integrating geophysical surface and depth information (Favetto *et al*. 2008; Perarnau *et al*. 2012; Orozco *et al*. 2013). The crustal structure shown is consistent with such data from other areas (Snyder, Ramos & Allmendinger, 1990; Comínguez & Ramos, 1991; Cristallini *et al*. 2004). Shallow seismicity data at *c*. 25 km (Richardson *et al*. 2013) indicate that the Sierras de Córdoba are accommodating current deformation in the most distant foreland portion of the Chilean trench. The presence of melted material associated with the Miocene magmatism and subsidence of the Pampia terrane – Río de la Plata craton interface is also detected (Booker, Favetto & Pomposiello, 2004).

In the west section B–B' (Fig. 5), a seismically active, almost vertical, planar structure which coincides with the Ojo de Agua lineament (Fig. 14a) is recognized based on seismic activity (Caro Montero, Martino & Guereschi, 2015). This lineament reaches a depth of *c*. 84 km, with sinistral transpressive kinematics (Fig. 14b, c). Despite the error range for hypocentral earthquake location of 3–5 km (depending on the database where data were obtained), such a structure is clearly detected although with a depth much greater than expected. In addition, from focal mechanisms calculated by the International Seismological Center for earthquakes located along this structure, a different kinematic style above and below the Mohorovicic discontinuity was deduced. The Ojo de Agua lineament has a transpressional nature with sinistral movement below this limit (*c*. 40 km) and reverse-type above it. This behaviour is possibly related to the rheological change between the lithosphere and the upper mantle. The same geometry is followed by the other oblique lineament on the east of section B–B' (Carapé).

The existence of ancient deep lineaments calls into question the geometry at depth, previously known or inferred, of the Sierras de Córdoba faults (Perarnau *et al*. 2012; Richardson *et al*. 2013; Martino, Guereschi & Caro Montero 2014, among others).

8. Regional interpretation: the case of the Sierra Chica fault

Although there are many studies still to be carried out on faults in the Sierras de Córdoba, one of the most studied faults, the Sierra Chica fault, can be taken as representative of the faulting affecting this part of the Sierras Pampeanas. In the Santa Rosa and El Tanque areas (Fig. 10b, c) there are excellent examples of basement thrusts produced during the Cenozoic deformation in the Sierras de Córdoba.

The brittle deformation in Sierra Chica produced a series of faults and lineaments with complex relationships (Fig. 3a). This complexity is due to the control exerted by previous fabrics such as the regional metamorphic foliation S_2 and locally the mylonitic

foliation in ductile shear zones, to which two overlapping brittle tectonic events can be added: the Cretaceous extensional tectonics and the Tertiary compressional tectonics.

The brittle deformation affected metamorphic rocks of Neoproterozoic–Cambrian ages (Rapela *et al*. 1998; Siegesmund *et al*. 2010) with a strong planar anisotropy that is very pervasive regionally (main metamorphic foliation S_2). This foliation has a general orientation N 310–340°/30–50° NE in Sierra Chica. The foliation S_2 is a plane of weakness and, in some places, acted as the main fault plane of the Sierra Chica fault (e.g. in the Santa Rosa area, Fig. 10c). The strong control exerted by the S_2 fabric of metamorphic rocks on the orientation of Tertiary brittle structures in the Eastern Sierras Pampeanas has been highlighted by many authors (Gordillo & Lencinas, 1979; Kraemer *et al*. 1988; Massabie & Szlafsztein, 1991; Kraemer & Martino, 1993; Schmidt *et al*. 1995; Simpson *et al*. 2001; Martino, Guereschi & Carignano, 2012). However, in other places the plane S_2 was cut at a low angle by the Sierra Chica fault plane (e.g. Villa Carlos Paz and Potrero de Garay areas, Fig. 12c, e). This case could also be interpreted as a shortcut imposed mechanically by a too-steep S_2 geometry, without significant rotation from inherited steeper faults to the shallow-dipping fault.

At the mountain scale, in the basement of Sierra Chica the fabric S_2 is cut by three N 330°-striking main oblique lineaments named, from north to south, Carapé, Quebrada Honda and Soconcho (Fig. 12a). These lineaments have a subvertical, straight trace on the map, and internally show an old mylonitic fabric and a superimposed new brittle fabric. The old fabric could be Devonian or older and later reactivated in a brittle regime during the Cretaceous and Tertiary tectonics. When the Tertiary compression occurred these lineaments were reactivated as dextral strike-slip faults, with an extensional component (divergent oblique shear = transtensive) generating drag and rotation of the fabric S_2 in the Quebrada Honda lineament and formation of cleavage superimposed on S_2 in the Carapé and Soconcho lineaments.

The oblique lineaments are here assigned to an old deformation, named pan-Gondwanan, which affected the South American and African plates (Daly, 1988; Tankard *et al*. 1995). As stated in Section 4, the relationship between the lineaments and the ductile shear zones is not clear; although they are commonly associated, not all the lineaments have mylonitic rocks linked to them. This is an open question currently under study.

The northern end of the Sierra Chica fault would have nucleated along the NW extension of the Carapé lineament (Fig. 12a). This would have been one of the main controls of the Cretaceous basin of the sierras of Pajarillo, Copacabana and Masa, because it is interpreted as the take-off listric normal fault (detachment or sole fault; Martino *et al*. 2014), then inverted during the Tertiary tectonics. An eroded harpoon-like structure (McClay & Buchanan, 1992) affecting the basal sedimentary sequence of the Cretaceous basin is recognized here and is one of the best places in the mountains to analyse the inversion of Cretaceous basins by Tertiary deformation. The Carapé and Guacha Corral–Pachango ductile shear zones (Fig. 4) are the two most important crustal boundaries in the Sierras de Córdoba, subsequent to the metamorphic peak and the beginning of exhumation of the Pampean orogen at this latitude (Martino, 2003).

High angles observed in some segments in the Sierra Chica fault plane, manifested as straight traces on the map (e.g. at the latitude of Cosquín, Fig. 12a), are interpreted as the result of translation and progressive back-rotation of the main fault as the imbrication of the sedimentary wedge occurred below (Fig. 11a). This implies an essentially non-rigid basement behaviour strongly influenced by the geometry of the footwall (Kraemer & Martino, 1993). Other straight segments of the Sierra Chica fault, that mark the boundaries of the Cretaceous basins sierras of Pajarillo, Copacabana and Masa in the north and Sierra de los Cóndores in the south (Fig. 4), are interpreted as Cretaceous normal faults today reversed by Tertiary tectonics. The curved segments are therefore new low-angle reverse faults (basement thrusts) caused by Tertiary tectonics, while the straight segments are rotated thrusts or reverse reactivations of previous faults as postulated in the Introduction section of this paper. Taken together, all segments are interconnected forming the current Sierra Chica fault.

In the segments between the oblique lineaments, the current Sierra Chica fault has a curved trace, convex westwards (salient S in Fig. 12a), while at the latitude of the lineaments the fault reverses becoming concave eastwards (recess R in Fig. 12a). The convex segments, limited by oblique lineaments, produced the segmentation of the Sierra Chica fault into at least three large thrusts sheets. During Tertiary compression, such sheets were displaced mainly towards the NNW (*c.* N 330°), while the lineaments acted as lateral ramps. The convex shape should be the effect of low-angle reverse faulting associated with the expansion of the front of the thrust sheet, a mechanism analogous to that recognized in the nappes (spreading nappes, Fig. 12g). The central fault segment between the Quebrada Honda and Soconcho lineaments can be taken as an example of the latter process and geometry. The thrust plane is slightly wavy, so locally the tectonic transport direction (arrows TTD in Fig. 12a) deviated from the main NNW-striking trend and veered to the west and SW. This gentle undulation of the fault plane is also observed at the latitude of Villa Carlos Paz, where it can be interpreted as a gently folded subvertical fault plane (Fig. 12c). An undulating fault plane is another factor that explains the various cross-cutting relationships observed with respect to the foliation plane S_2 (Fig. 3f).

Kinematic analysis of minor faults in the areas of Cosquín, Villa Carlos Paz and Santa Rosa (Kraemer *et al*. 1988; Kraemer & Martino, 1993; Painceyra, 1998) indicates that there are two common directions of

shortening that belong to different deformation events, NW and NE, corresponding to events A and B, respectively (Fig. 12b, d). It is worth noting that recent focal mechanisms, deduced by P and S waves, are coincident with the event A since a component of NW shortening and subvertical lengthening (Richardson *et al*. 2009) is determined. This dynamic also coincides with the determined main direction of tectonic transport (TTD arrows, Fig. 12a) for the various blocks of the Sierra Chica limited by the Carapé, Quebrada Honda and Soconcho lineaments.

The Tertiary reverse fault of Sierra Chica was nucleated and reactivated, and then inverted a Cretaceous normal fault related to the deformation that led to the opening of the Atlantic Ocean (Schmidt *et al*. 1995). This coincides with the Eastern Pampean lineament (Fig. 1) corresponding to the suture produced by the assembly of the Río de la Plata craton with the Pampia terrane in Precambrian times. The latter lineament and the current fault are probably the surface expression of the true suture, now in lower structural levels of the lithosphere but geophysically detected (Booker, Favetto & Pomposiello, 2004; Gilbert *et al*. 2010).

Based on geobarometric data obtained from metamorphic rocks of the blocks exhumed on both sides of the Sierra Chica fault, Martino, Guereschi & Carignano (2011) estimated a throw of between *c.* 5 km at Alta Gracia (31° 36′ S) and *c.* 12 km at La Calera (31° 21′ S). This present-day geobarometric difference is an effect of Cretaceous extensional tectonics that was not compensated by the Tertiary inversion.

9. Considerations about the age of faulting

Based on thermochronological data that indicate activity as early as during the Carboniferous period, the inversion of the Cretaceous basin and Cenozoic synorogenic deposits affected by subsequent faulting, it can be deduced that block uplift resulted from different orogenic cycles from the Palaeozoic era to present times. It should be noted that the modern mountain uplift is not recorded by thermochronological data, but it can be constrained based on stratigraphic evidence from the overthrust sequences and their regional correlation. The information available is fragmentary, the Sierra de Pocho, Sierra de Comechingones and Sierra Chica faults being the best studied to date.

Based on radiometric dating in pseudotachylites from the Sierra de Pocho fault (Fig. 4), the deformation could have been active from the early Carboniferous period (*c.* 350–340 Ma, Whitmeyer, 2008). Brittle reactivation of this structure with development of gouge and brecciation is probably linked to the Cenozoic deformation that produced the uplift of the sierras of Guasapampa and Pocho. The origin of the large asymmetrical synformal fold in sedimentary rocks (a drag fold?) could be a concomitant event. The magmatism associated with the Andean orogenic cycle, represented by the Pocho Volcanic Complex (7.9–4.7 Ma; Kay & Gordillo, 1994; Arnosio *et al*. 2014) and in the Sierra del Morro at San Luis (2.6 ± 0.7 Ma and 1.9 ± 0.2 Ma; Ramos, Munizaga & Kay, 1991). The Pocho volcanic rocks overlying the eastern flank of the Sierra de Pocho show strong erosion on the west side near the top of the sierra. This would indicate that these rocks were tilted to the east, probably as a result of the reactivation of the Sierra de Pocho fault during Pliocene–Pleistocene times.

For the Sierra de Comechingones fault, based on the results of K–Ar fault gouge dating, Bense *et al.* (2011) set the onset of brittle deformation as early Carboniferous (*c.* 340 Ma) followed by Permian–Triassic and Jurassic events. Löbens *et al*. (2011) proposed that the current structural relief was achieved after the late Cretaceous exhumation (*c.* 80–70 Ma, based on thermochronological data). This fault also recorded Quaternary activity dated at 7.1 ± 0.4 ka and 350 ± 40 ka BP (the El Molino fault, Fig. 4; Costa *et al.* 2014).

The Sierra Chica fault is a Tertiary reverse fault that was nucleated and reactivated and then inverted a normal fault of the Cretaceous rift. To date, thermochronological data are not available to constrain previous brittle activity. The age of the Cenozoic deformation depends on the age assigned to the sedimentary sequences overthrust by the basement. In the Cosquín area, the Eocene–Oligocene Cosquín Formation is separated by a calcrete horizon from the Miocene–Pliocene Casagrande Formation, and both sequences were imbricated by reverse-faulting (Fig. 11a) during the Pliocene–Pleistocene periods. In the Santa Rosa area (Fig. 11b), deformation event A is clearly recognized in clay levels in the fault plane suggesting that it was the last episode of movement, probably post-Pliocene (early Pleistocene?). Event B is recognized in the basement relatively far from the fault plane and is considered as a previous event of uncertain age (pre-late Pliocene?, Kraemer *et al*. 1988). Both events coincide approximately with the Pliocene–Pleistocene imbrication of the Cosquín and Casagrande formations. According to Schmidt *et al*. (1995), deformation developed after the Pliocene period based on the inversion of the Cretaceous basins. Based on stratigraphic evidence in the Sierras de Córdoba and correlation with structural analysis in the Puna and northwestern Sierras Pampeanas (Allmendinger, 1986; Marrett & Allmendinger, 1987), Martino *et al*. (1995) proposed that the two deformational events occurred during the Pleistocene, at *c.* 0.8 Ma (event A) and *c.* 2 Ma (event B). In addition, very recent (Holocene?) displacements have been recognized (Costa *et al.* 2014) based on geomorphology and observations of soil horizons affected by the faulting (e.g. in the Potrero de Garay area). Reactivation of the Sierra Chica fault therefore developed during late Pliocene – Pleistocene – Holocene times. In addition, southwards diachronism in fault propagation is recognized based on the overthrust relationship over younger sedimentary rocks to soils in that direction.

The age of the reactivation of the easternmost Elevación Pampeana fault is unknown, but it is estimated to be more recent than the Sierra Chica fault. Other

authors (Costa & Vita-Finzi, 1996; Costa *et al*. 2001) believe that it is a Holocene uplift but with variable uplift rates.

Seismological and seismic risk features linked to the latest deformation have been recently reviewed by Fatala & Martino (2012), Perarnau *et al*. (2012), Costa *et al*. (2014) and Caro Montero, Martino & Guereschi (2015). The Ciénaga del Coro fault, Ojo de Agua lineament, La Sierrita fault, northern segments of the Cumbre de Gaspar and Sierra Chica faults all exhibit present-day seismic activity, with magnitudes of 2–4 (M_b).

The synorogenic deposits in the piedmont of the Sierra Chica fault (Fig. 11a) and the interception of drainage from Sierra Grande by Sierra Chica provide clear evidence of uplift of the Sierra Grande prior to that of Sierra Chica through its eponymous faults.

Based on thermochronometric data of apatite and zircon (U/Th)/He ages, Richardson *et al*. (2013) postulated Permian – Early Jurassic cooling in the basement of the Sierras de Córdoba, suggesting that exhumation has been less than 2–3 km since then. Faulting and uplift in the Sierras Pampeanas of Córdoba is diachronous from north to south, based on the overthrusting relationship in sedimentary sequences and thermochronological data. This suggests discrete block uplift, reflecting segmentation produced partly by the oblique lineaments and partly by other ancient faults. The fault reactivation would have formed mountain ranges internally composed of blocks that rose diachronously.

The direction of propagation of the main faults with a dominant westerly vergence was from west to east (backwards propagation), with the Río de La Plata craton acting as a buttress. The present topography is the result of the Permian – Early Jurassic exhumation (according to (U/Th)/He data) plus the Pliocene–Quaternary uplift of *c.* 2–3 km, not detected by thermochronometric data as in most of the Sierras Pampeanas. In addition, palaeoclimatic and geomophological observations allow the remnants of pre-Cenozoic landforms to be recognized (Rabassa *et al*. 1997; Carignano, Cioccale & Rabassa, 1999).

10. Concluding remarks

The Sierras Pampeanas de Córdoba are the easternmost uplift blocks related to current Andean foreland deformation, over 700 km from the Chilean trench and coinciding with a region of low inclination and shallowing of subduction of the Nazca plate beneath the South American plate (the Pampean flat-slab). By coupling between the two plates, this phenomenon has been compared to the Laramide orogeny of North America and elsewhere in the world (Jordan *et al*. 1983*b*; Rodgers, 1987; Marshak, Karsltrom & Timmons, 2000). In the Sierras Pampeanas, it occurs between 27° and 34° S latitude and was active from 12 Ma to the present (Ramos & Folguera, 2009), causing thick-skinned tectonics over an area of about 800×600 km.

At the latitude of the Sierras de Córdoba, the top of the Nazca plate is located at a depth of *c.* 175 km (Cahill & Isacks, 1992; Booker, Favetto & Pomposiello, 2004), as detected by seismic and magnetotelluric surveys. These studies also suggested that, towards the east of Sierra Chica (Alta Gracia, Fig. 4), almost vertical sinking of the Nazca plate would occur, probably related to the presence of the western boundary of the Río de la Plata craton (Rapela *et al*. 2007).

The asymmetric uplift blocks of the Sierras de Córdoba are arranged in N–S-aligned ranges limited by E-dipping reverse faults, both high- and low-angle, with a steep western flank and a gentle eastern flank (e.g. 10–12° for Sierra Chica). Looking to the north, there is clockwise tilting. Four blocks are distinguished from west to east: Sierra de Pocho; Sierra de Comechingones–Grande (highest elevation Cerro Champaquí: 2884 m a.s.l.); Sierra Chica (Cerro Uritorco: 1950 m a.s.l.); and Elevación Pampeana. Between the blocks are Mesozoic and Cenozoic basins, the latter partitioned by the deformation that uplifted the blocks from *c.* 10 Ma ago (Jordan *et al*. 1989; Schmidt *et al.* 1995; Ramos, 1999). These basins were covered by Pleistocene rocks and Holocene soils in turn. Data from depth of the Mohorovicic discontinuity and thermochronometric dating indicate Permian – Early Jurassic cooling, suggesting that exhumation has been less than 2–3 km since then (Richardson *et al*. 2013). An even older age (Carboniferous) has been proposed, so the current relief could have partial Palaeozoic and Mesozoic inheritance and was not only produced by the Andean orogeny (Jordan *et al*. 1989; Coughlin *et al.* 1998; Löbens *et al*. 2011; Martino, Guereschi & Carignano, 2012).

The controls on the Andean deformation by faulting in the Sierras de Córdoba are varied: (1) the dominant basement metamorphic fabric S_2 (Kraemer *et al*. 1988; Kraemer, Escayola & Martino, 1995; Martino, Guereschi & Carignano, 2012); (2) the reactivation of suture zones (Schmidt *et al*. 1995); and (3) the reactivation of Cretaceous normal faults (Martino, Guereschi & Carignano, 2012). We recognize two further factors. (4) Based on geological and geophysical data, we propose that oblique lineaments are another kind of control on the nucleation and development of Tertiary faulting. These lineaments are old, probably correlated with the pan-Gondwanan trend (Daly, 1988; Tankard *et al*. 1995) and deeply affect the crust, shifting the Mohorovicic discontinuity (Perarnau *et al*. 2012). They worked in a transtensional way (= divergent oblique shear) during the Cretaceous period, uplifting high-grade metamorphic rocks in their highest parts during Cenozoic tectonics (Martino, Guereschi & Carignano, 2012). These lineaments are also the locus of magmas represented by Paleocene olivine nephelinites dykes and serve as metallotects for gold and uranium mineralization. The Ojo de Agua lineament (Fig. 4), one of these ancient lineaments, extends to the SE into the Soconcho lineament, forming a single structure at regional scale, with deep current seismic activity

below the Mohorovicic discontinuity to *c.* 80 km (Caro Montero, Martino & Guereschi, 2015). (5) Finally, there is clear control exerted by Palaeozoic ductile shear zones in both the hangingwall and footwall on the Tertiary brittle deformation. As an example, the Pachango lineament and the eponymous ductile shear zone (Fig. 7a) make the southern boundary of the large Los Túneles shear zone and put rocks with contrasting metamorphic grades into contact.

According to observations in many places, it has been traditionally considered that in the Sierras Pampeanas high-angle reverse faults limit mountain range blocks (González Bonorino, 1950; Gordillo & Lencinas, 1979). However, in some places very-low-angle reverse faults (thrusts) also produced block uplifts. The block of the Sierra Chica is an example of these different angles of faulting. As described, the Sierra Chica fault has a sinuous trace with straight and curved segments. The straight segments have high angles and are associated with inverted Cretaceous basins, whose remains lie on top of the uplifted blocks. Other straight segments would be rotated basement thrusts as the result of translation and progressive back rotation of the main fault, as the imbrication of the sedimentary wedge occurs below (Fig. 11a). This implies a basement behaviour that is essentially non-rigid and strongly influenced by the geometry of the footwall (Kraemer & Martino, 1993). All straight segments are connected by curved segments, which have a lower angle, are younger and are where true basement thrust is recognized (e.g. areas of Villa Carlos Paz and Santa Rosa; Fig. 6).

Dominantly W-vergent with sequential hangingwall faulting propagated from west to east (backwards faulting propagation), with the Río de la Plata craton as a buttress located to the east and deep in the Chaco-Pampean plain.

The overthrust relationships in sedimentary sequences and thermochronological data indicate discrete block uplift, reflecting segmentation produced partly by the oblique lineaments and partly by ancient faults. Fault reactivation formed mountain ranges internally composed of blocks that rose diachronously.

The uplift of the blocks and the maximum displacement estimated by the bow-and-arrow method (Elliott, 1976) decrease in the same direction, from 8.8 km in the west to 3.2 km in the east, with a displacement/length ratio varying from 1:12 and 1:6 and with an average value of 1:8.4 ($\gamma = 0.13$). The tectonic transport direction is relatively constant, with values of N 260–270°.

Quaternary movements are recognized in the El Molino fault near Merlo and in the Sierra Chica fault (Costa & Vita-Finzi, 1996; Costa *et al*. 2001). The fault that uplifted the Sierra Baja de San Marcos provides evidence for neotectonic activity in two stages during late Holocene time (Massabie, 1982; Massabie *et al.* 2003); for a detailed review of the neotectonic activity see Costa *et al*. (2014). At the present time, the latest deformation is registered by seismic activity, showing magnitudes (M_b) of 2–4.

Acknowledgements. The CONICET, FONCyT, SECyT–UNC and Secretaría de Minería of the Province of Córdoba (Argentina) institutions are thanked for supporting our research over the years. Formal revisions by two referees, V. Ramos and an anonymous reviewer, and the editorial assistance of O. Lacombe are acknowledged for their contributions which significantly improved the manuscript. Language revision by R. J. Pankhurst is gratefully acknowledged.

References

ALLMENDINGER, R.W. 1986. Tectonic development, southeastern border of the Puna Plateau, northwestern Argentine Andes. *Bulletin of the Geological Society of America* **97**(9), 1070–82.

ALVARADO, P., BECK, S., ZANDT, G., ARAUJO, M. & TRIEP, E. 2005. Crustal deformation in the south-central Andes backarc terranes as viewed form regional broad-band seismic waveform modelling. *Geophysical Journal International* **163**, 580–98.

ALVARADO, P., MACHUCA, B. G. & BECK, S. 2005. Comparative seismic and petrographic crustal study between the Western and Eastern Sierras Pampeanas region (31º S). *Revista de la Asociación Geológica Argentina* **60**, 787–96.

ARNOSIO, M., POPRIDKIN, C., BÁEZ, W. & BUSTOS, E. 2014. El volcanismo terciario: Complejo Volcánico Pocho. In *Geología y Recursos Naturales de la Provincia de Córdoba* (eds R. D. Martino & A. B. Guereschi), pp. 623–47. Relatorio del 19º Congreso Geológico Argentino, Asociación Geológica Argentina, Córdoba.

ASSUMPÇÃO, M., FENG, M. & JULIÀ, J. 2013. Models of crustal thickness for South America from seismic refraction, receiver functions and surface wave tomography. *Tectonophysics* **609**, 82–96.

BEDER, R. 1922. Estudios geológicos en la Sierra de Córdoba, especialmente de las calizas cristalino-granulosas y sus fenómenos de metamorfismo. Dirección de Minas, Geología e Hidrogeología, Boletín 33, Serie B, Buenos Aires.

BENSE, F. A., LÖBENS, S., DUNKL, I. & WEMMER, K. 2013. Is the exhumation of the Sierras Pampeanas only related to Neogene flat-slab subduction? Implications from a multi-thermochronological approach. *Journal of South American Earth Science* **48**, 123–44.

BENSE, F.A., LÖBENS, S., WEMMER, K., DUNKL, I., COSTA, C. H., LAYER, P. & SIEGESMUND, S. 2011. K-Ar fault gouge dating in the Sierra de Comechingones (Argentina). *18º Congreso Geológico Argentino*, Actas, pp. 144–145. Neuquén.

BERTOLINO, S. R. A. & MURRAY, H. H. 1992. La mina Eureka (Provincia de Córdoba): un depósito excepcional de illita. *Revista de la Asociación Geológica Argentina* **47**, 113–4.

BLASÓN, R. 1999. Yacimiento Schlagintweit, distrito minero uranífero Batolito de Achala, Córdoba. In *Recursos Minerales de la República Argentina* (ed. E. O. Zappettini), pp. 613–20. Instituto de Geología y Recursos Minerales, SEGEMAR, Anales no. 35, Buenos Aires.

BODENBENDER, G. 1929. Triásico y Terciario de la falda oriental de la Sierra de Córdoba. Relaciones morfológico-tectónicas. Rocas volcánicas. *Boletín de la Academia Nacional de Ciencias* **31**, 73–139, Córdoba.

BOOKER, J., FAVETTO, A. & POMPOSIELLO, C. 2004. Low electrical resistivity associated with plunging of the Nazca flat slab beneath Argentina. *Nature* **429**, 399–403.

BOYER, S. & ELLIOT, D. 1982. Thrust systems. *The American Association of Petroleum Geologist Bulletin* **66**, 1196–230.

BULL, W. B. 2007. *Tectonic Geomorphology of Mountains: A New Approach to Paleoseismology*. Oxford: Blackwell Publishing, 316 pp.

CAHILL, T. & ISACKS, B. L. 1992. Seismicity and shape of the subducted Nazca plate. *Journal of Geophysical Research* **97** (B12), 17 503–17 529.

CARIGNANO, C., CIOCCALE, M. & RABASSA, J. 1999. Landscape antiquity of the Central Eastern Sierras Pampeanas (Argentina): Geomorphological evolution since Gondwanic times. *Zeitschrift für Geomorphologie*, NF, Supplement Band **118**, 245–68.

CARO MONTERO, A., MARTINO, R. D. & GUERESCHI, A. B. 2015. Estudio sismotectónico integrado de la falla Ciénaga del Coro, lineamiento Ojo de Agua y falla La Sierrita, Sierras de Córdoba. *16º Reunión de Tectónica*, Resúmenes, pp. 186–7, General Roca.

CASTELLANOS, A. 1944. Paleontología estratigráfica de los sedimentos neógenos de la provincia de Córdoba. *Publicaciones del Instituto de Fisiografía y Geología de la Universidad Nacional del Litoral* **23**, 5–47.

CASTELLANOS, A. 1951. Un nuevo género de Esclerocaliptino ("Isolinia") descubierto en el araucaniano del Valle de Los Reartes (Sierras de Córdoba). *Revista de la Asociación Geológica Argentina* **6**, 95–100.

CHEBLI, G. A., SPALLETTI, L. A., RIVAROLA, D., DE ELORRIAGA, E. & WEBSTER, R. E. 2005. Cuencas cretácicas de la región central de la Argentina. In *Simposio Frontera Exploratoria de la Argentina* (eds G. Chebli, J. Cortiñas, L. Spalletti, L. Legarreta & E. Vallejo), pp. 193–215. Actas 6º Congreso de Exploración y Desarrollo de Hidrocarburos, Chapter 9, Buenos Aires.

CHERNICOFF, C. J. & RAMOS, V. A. 2003. El basamento de la Sierra de San Luis. Nuevas evidencias magnéticas y sus implicancias tectónicas. *Revista de la Asociación Geológica Argentina* **58**(4), 511–24.

COMÍNGUEZ, A. H. & RAMOS, V. A. 1991. La estructura profunda entre Precordillera y Sierras Pampeanas de la Argentina: evidencias de la sísmica de reflexión profunda. *Revista Geológica de Chile* **18**, 3–14.

COSTA, C. H., MASSABIE, A. C., SAGRIPANTI, G. L., BRUNETTO, E. & COPPOLECCHIA, M. 2014. Neotectónica. In *Geología y Recursos Naturales de la Provincia de Córdoba* (eds R. D. Martino & A. B. Guereschi), pp. 725–46. Relatorio del 19º Congreso Geológico Argentino, Asociación Geológica Argentina, Córdoba.

COSTA, C., MURILLO, V., SAGRIPANTI, G. & GARDINI, C. 2001. Quaternary intraplate deformation in the southeastern Sierras Pampeanas, Argentina. *Journal of Seismology* **5**, 399–409.

COSTA, C. H. & VITA-FINZI, C. 1996. Late Holocene faulting in the southeast Sierras Pampeanas of Argentina. *Geology* **24**, 1127–30.

COUGHLIN, T. J., O'SULLIVAN, P. B., KHON, B. P. & HOLCOMBE, R. J. 1998. Apatite fission-track thermochronology of the Sierras Pampeanas, central western Argentina: implications for the mechanism of plateau uplift in the andes. *Geology* **26**, 999–1002.

COWIE, P. A. 1998. Normal growth fault in three-dimensions in continental and oceanic crust. In *Faulting and Magmatism at Mid-Ocean Ridges* (eds W. R. Buck, P. T. Delaney, J. A. Karson & Y. Lagabrielle), pp. 325–48. American Geophysical Union, Washington, Geophysical Monograph no. 106.

CRISTALLINI, E. O., COMINGUEZ, A. H., RAMOS, V. A. & MERCERAT, E. D. 2004. Basement double-wedge thrusting in the northern Sierras Pampeanas of Argentina (26° S): constraints from deep seismic reflection. In *Thrust Tectonics and Hydrocarbon Systems* (ed K. R. Mc Clay), pp. 65–90. American Association of Petroleum Geologists, Memoir no. 82.

CUERDA, A. 1973. Sierras Pampeanas, una nueva interpretación de su estructura. *Revista de la Asociación Geológica Argentina* **38**, 293–303.

DALY, M. C. 1988. Crustal shear zones in Central Africa: a kinematic approach to Proterozoic tectonics. *Episodes* **11**, 5–11.

ELLIOTT, D. 1976. The motion of thrust sheets. *Journal of Geophysical Research* **81**, 949–63.

FATALA, J. M. & MARTINO, R. D. 2012. Mapa sísmico y evaluación de peligro sísmico en las Sierras Pampeanas de Córdoba y San Luis. *15º Reunión de Tectónica*, Libro de Resúmenes, San Juan, p. 48.

FAVETTO, A., POMPOSIELLO, C., LÓPEZ DE LUCHI, M. G. & BOOKER, J. 2008. 2D Magnetotelluric interpretaion of the crust electrical resistivity across the Pampean terrane – Río de la Plata suture, in central Argentina. *Tectonophysics* **459**, 53–65.

GILBERT, H., BECK, S. & ZANDT, G. 2006. Lithospheric and upper mantle structure of central Chile and Argentina. *Geophysical Journal International* **165**, 383–98.

GILBERT, H. J., RICHARDSON, T. J., ANDERSON, M. L., ALVARADO, P. M., MARTINO, R. D., BECK, S. L., ZANDT, G. & GANS, C. 2010. Active deformation in the Sierras de Córdoba: Observations from the Eastern Sierras Pampeanas seismic array. *EOS Transactions* AGU, The Meeting of the Americas 2010, Foz do Iguazu, Abstract S22A–05.

GONZÁLEZ BONORINO, F. 1950. Algunos problemas geológicos de las Sierras Pampeanas. *Revista de la Asociación Geológica Argentina* **5**, 8–110.

GORDILLO, C. E. & LENCINAS, A. N. 1979. Sierras Pampeanas de Córdoba y San Luis. In *Segundo Simposio de Geología Regional Argentina* (ed. J. C. Turner), pp. 577–650. Academia Nacional de Ciencias, Córdoba.

GORDILLO, C. E., LINARES, E. & DAZIANO, C. O. 1983. Nuevo afloramiento de nefelinita olivínica: Estancia Guasta, Sierra de Córdoba. *Revista de la Asociación Geológica Argentina*, **38**, 485–9.

GROSHONG, R. H. 2008. *3-D Structural Geology: A Practical Guide to Quantitative Surface and Subsurface Map Interpretation*. Second edition. Berlin: Springer-Verlag, 400 pp.

GROSS, W. 1948. Cuadro tectónico del valle de Punilla. *Revista de la Asociación Geológica Argentina* **3**, 73–132.

GUERESCHI, A. B. & MARTINO, R. D. 2014. Las migmatitas de las Sierras de Córdoba. In *Geología y Recursos Naturales de la Provincia de Córdoba* (eds R. D. Martino & A. B. Guereschi), pp. 67–94. Relatorio del 19º Congreso Geológico Argentino. Córdoba: Asociación Geológica Argentina.

HEIT, B., YUAN, X., BIANCHI, M., SODOUDI, F. & KIND, R. 2008. Crustal thickness estimation beneath the southern central Andes at 30º S and 36º S from S wave receiver function analysis. *Geophysical Journal International* **174**, 249–54.

INTROCASO, A., LION, A. L. & RAMOS, V. 1987. La estructura profunda de las Sierras de Córdoba. *Revista de la Asociación Geológica Argentina* **13**, 177–87.

JORDAN, T. & ALLMENDINGER, R. 1986. The Sierras Pampeanas of Argentina. A modern analogue of Rocky Mountain foreland deformation. *American Journal of Science* **286**, 737–64.

JORDAN, T. E., ISACKS, B. L., ALLMENDINGER, R. W., BREWER, J. A., RAMOS, V. A. & ANDO, C. J. 1983a. Andean tectonics related to the geometry of the subducted Nazca Plate. *Geological Society of America Bulletin* **94**, 341–61.

JORDAN, T. E., ISACKS, B. L., RAMOS, V. A. & ALLMENDINGER, R. W. 1983b. Mountain building in the Central Andes. *Episodes* **3**, 20–6.

JORDAN, T., ZEITLER, P., RAMOS, V. & GLEADOW, A. 1989. Thermochronometric data on the development of the basament peneplain in the Sierras Pampeanas, Argentina. *Journal of South American Earth Science* **2**, 207–22.

KAY, S. M. & GORDILLO, C. E. 1994. Pocho volcanic rocks and the melting of depleted continental lithosphere above a shallowly dipping subduction zone in the central Andes. *Contributions to Mineralogy and Petrology* **117**, 25–44.

KRAEMER, P., ESCAYOLA, M. & MARTINO, R. 1995. Hipótesis sobre la evolución tectónica neoproterozoica de las Sierras Pampeanas de Córdoba (30º 40′ LS – 32º 40′ LS). *Revista de la Asociación Geológica Argentina* **50**, 47–59.

KRAEMER, P. & MARTINO, R. 1993. La falla de la Sierra Chica, cabalgamiento de basamento sobre una cuña sedimentaria imbricada, Cosquín. *9º Reunión sobre Microtectónica*, Actas, Mendoza, pp. 13–14.

KRAEMER, P., MARTINO, R., GIAMBASTIANI, M. & SFRAGULLA, J. 1988. Análisis dinámico-cinemático preliminar de la Falla de Santa Rosa, Dpto. de Calamuchita, prov. de Córdoba. *5º Reunión de Microtectónica*, Actas, Córdoba, pp. 107–20.

KRAEMER, P., TAUBER, A., SCHMIDT, C. & RAMÉ, G. 1993. Análisis cinemático de la falla de Nono, evidencias de actividad neotectónica, Valle de San Alberto. Provincia de Córdoba. *12º Congreso Geológico Argentino y 2º Congreso de Exploración de Hidrocarburos*, Actas 3, Mendoza, pp. 277–81.

LAGORIO, S. L., VIZÁN, H. & GEUNA, S. E. 2014. El volcanismo alcalino cretácico. In *Geología y Recursos Naturales de la Provincia de Córdoba* (eds R. D. Martino & A. B. Guereschi), pp. 473–511. Relatorio del 19º Congreso Geológico Argentino. Córdoba: Asociación Geológica Argentina.

LENCINAS, A. & TIMONIERI, A. 1968. Algunas características estructurales del Valle de Punilla, Córdoba. *3º Jornadas Geológicas Argentinas*, Actas 1, Buenos Aires, pp. 195–208.

LINARES, E., TIMONIERI, A. J. & PASCUAL, R. 1960. La edad de los sedimentos terciarios del Valle de Punilla, Provincia de Córdoba, y la presencia de "Eohyrax Rusticus" Ameghino en los mismos. *Revista de la Asociación Geológica Argentina* **15**, 191–210.

LÖBENS, S., BENSE, F. A., WEMMER, K., DUNKL, I., COSTA, C. H., LAYER, P. & SIEGESMUND, S. 2011. Exhumation and uplift of the Sierras Pampeanas: preliminary implications from K–Ar fault gouge dating and low-Tthermochronology in the Sierra de Comechingones (Argentina). *International Journal of Earth Sciences* **100**, 671–94.

LUCERO MICHAUT, H. N. 1976. Las estructuras plegadas de los sedimentos terciarios del Valle de Punilla. *Boletín de la Academia Nacional de Ciencias* **51**, 265–81.

LUCERO MICHAUT, H. & OLSACHER, J. 1981. Descripción geológica de la Hoja 19 h, Cruz del Eje. Servicio Geológico Nacional, Boletín no. 179, 1–96. Buenos Aires.

MARRETT, R. A. & ALLMENDINGER, R. W. 1987. La cinemática de fallas y su relación con el volcanismo andino del valle Calchaquí norte. In *X Congreso Geológico Argentino* **1**, 223–6.

MARRETT, R. & ALLMENDINGER, R. 1990. Kinematic analysis of fault slip data. *Journal of Structural Geology* **12**, 937–86.

MARSHAK, S., KARSLTROM, K. & TIMMONS, J. M. 2000. Inversion of Proterozoic extensional faults: an explanation for the pattern of Laramide and Ancestral Rockies intracratonic deformation, United States. *Geology* **28**, 735–8.

MARTINO, R. D. 2003. Las fajas de deformación dúctil de las Sierras Pampeanas de Córdoba: una reseña general. *Revista de la Asociación Geológica Argentina* **58**, 549–71.

MARTINO, R. D. & GUERESCHI, A. B. 2014. La estructura neoproterozoica–paleozoica inferior del complejo metamórfico de las Sierras de Córdoba. In *Geología y Recursos Naturales de la Provincia de Córdoba* (eds R. D. Martino & A. B. Guereschi), pp. 95–128. Relatorio del 19º Congreso Geológico Argentino. Córdoba: Asociación Geológica Argentina.

MARTINO, R. D., GUERESCHI, A. B. & CARIGNANO, C. C. 2011. Geobarometría en gneises del techo y el piso de la falla de la Sierra Chica y su relación con la tectónica y cuencas cretácicas, Sierras de Córdoba, Argentina. *8º Congreso de Exploración y Desarrollo de Hidrocarburos*, Mar del Plata. Trabajos Técnicos: 251–63. Instituto Argentino del Petróleo y el Gas, Buenos Aires.

MARTINO, R. D., GUERESCHI, A. B. & CARIGNANO, C. C. 2012. Influencia de la tectónica Preandina sobre la tectónica Andina: El caso de la falla de la Sierra Chica, Sierras Pampeanas de Córdoba. *Revista de la Asociación Geológica Argentina* **69**, 207–21.

MARTINO, R. D., GUERESCHI, A. B., CARIGNANO, C. A., CALEGARI, R. J. & MANONI, R. 2014. La estructura de las cuencas extensionales cretácicas de las Sierras de Córdoba. In *Geología y Recursos Naturales de la Provincia de Córdoba* (eds R. D. Martino & A. B. Guereschi), pp. 513–38. Relatorio del 19º Congreso Geológico Argentino. Córdoba: Asociación Geológica Argentina.

MARTINO, R. D., GUERESCHI, A. B. & CARO MONTERO, A. 2014. La estructura cenozoica (paleógena–neógena) de las Sierras de Córdoba. In *Geología y Recursos Naturales de la Provincia de Córdoba* (eds R. D. Martino & A. B. Guereschi), pp. 649–71. Relatorio del 19º Congreso Geológico Argentino. Córdoba: Asociación Geológica Argentina.

MARTINO, R. D., GUERESCHI, A. B. & SFRAGULLA, J. A. 2002. Deformación frágil y relaciones regionales de la Faja de Deformación Los Túneles en las sierras de Pocho y Guasapampa, Córdoba, Argentina. *15º Congreso Geológico Argentino*, Actas 1, El Calafate, pp. 232–7.

MARTINO, R., KRAEMER, P., ESCAYOLA, M., GIAMBASTIANI, M. & ARNOSIO, M. 1995. Transecta de las Sierras Pampeanas de Córdoba a los 32º LS. *Revista de la Asociación Geológica Argentina* **50**, 60–77.

MARTINO, R. D., TOLEDO, A. E. & GUERESCHI, A. B. 2012. Lineamientos transtensionales en el margen noroccidental del batolito de Achala y su relación con la exhumación de rocas de alto grado y la extensión cretácica en las Sierras de Córdoba. *15º Reunión de Tectónica*, Libro de Resúmenes, San Juan, p. 90.

MASSABIE, A. 1976. Estructura cenozoica entre Charbonier y Cosquín, provincia de Córdoba. *6º Congreso Geológico Argentino*, Actas 1, Tucumán, 195–208.

MASSABIE, A. 1982. Geología de los alrededores de Capilla del Monte y San Marcos, Provincia de Córdoba. *Revista de la Asociación Geológica Argentina* **37**, 153–73.

MASSABIE, A. 1987. Neotectónica y sismicidad en la región de las Sierras Pampeanas orientales, Sierras de Córdoba, Argentina. *10º Congreso Geológico Argentino*, Actas 1, Tucumán, pp. 271–4.

MASSABIE, A., SANGUINETTI, A., LO FORTE, G. & CEGARRA, M. 2003. La actividad neotectónica en la Sierra Baja de San Marcos – Cruz del Eje, flanco occidental de las Sierras Pampeanas Orientales. *Revista de la Asociación Geológica Argentina* **58**, 653–63.

MASSABIE, A. & SZLAFSZTEIN, C. 1991. Condiciones geomecánicas y edad del fallamiento neotectónico en las Sierras Pampeanas Orientales, Córdoba, Argentina. *Asociación Argentina de Geología Aplicada a la Ingeniería*, Actas **6**, 154–68.

MCCLAY, K. R. & BUCHANAN, P. G. 1992. Thrust faults in inverted extensional basins. In *Thrust Tectonics* (ed. K. R. McClay), pp. 419–34. London: Chapman & Hall.

OLSACHER, J. 1972. Descripción geológica de la Hoja 21h, Cerro Champaquí, Provincia de Córdoba. *Dirección Nacional de Geología y Minería, Boletín* **133**, 1–64.

OROZCO, L. A., FAVETTO, A., POMPOSIELLO, C., ROSSELLO, E. & BOOKER, J. 2013. Crustal deformation of the Andean foreland at 31º 30′ S (Argentina) constrained by magnetotelluric survey. *Tectonophysics* **582**, 126–39.

PAINCEYRA, R. 1998. Estudio estructural de la Falla de Punilla en Villa Carlos Paz, Sierra Chica de Córdoba, Argentina. *10º Congreso Geológico Latinoamericano de Geología y 6º Congreso Nacional de Geología Económica*, Actas 1, Buenos Aires, pp. 183–8.

PERARNAU, M., ALVARADO, P. & SAEZ, M. 2010. Estimación de la estructura cortical de velocidades sísmicas en el suroeste de la Sierra de Pie de Palo, provincia de San Juan. *Revista de la Asociación Geológica Argentina* **67**(4), 473–80.

PERARNAU, M., GILBERT, H., ALVARADO, P., MARTINO, R. & ANDERSON, M. 2012. Crustal structure of the Eastern Sierras Pampeanas of Argentina using high frequency local receiver functions. *Tectonophysics* **580**, 208–17.

RABASSA, J., ZARATE, M., PARTRIDGE, T. C., MAUD, R., CIOCCALE, M. & CARIGNANO, C. 1997. Gondwanic relict paleolandscapes in cratonic areas of Argentina. *4º International Conference on Geomorphology Abstracts*, Supplementi di Geografia Fisica e Dinamica Quaternaria, Supplement 3, 1: 321, Torino.

RAMOS, V. A. 1988. Late Proterozoic –Early Paleozoic of South America – a collisional history. *Episodes* **11**(3), 168–74.

RAMOS, V. A. 1999. Los depósitos sinorogénicos terciarios de la region andina. Geología Argentina. In *Geología Argentina* (ed. R. Caminos), pp. 651–82. Instituto de Geología y Recursos Minerales, Buenos Aires, Anales no. 29.

RAMOS, V. A., CRISTALLINI, E. O. & PÉREZ, D. J. 2002. The Pampean flat-slab of the Central Andes. *Journal of South American Earth Sciences* **15**, 59–78.

RAMOS, V. A., ESCAYOLA, M., MUTTI, D. & VUJOVICH, G. I. 2000. Proterozoic–early Paleozoic ophiolites in the Andean basement of southern South America. In *Ophiolites and Oceanic Crust: New Insights from Field Studies and Ocean Drilling Program* (eds Y. Dilek & E. Moores), pp. 331–49. Geological Society of America, Boulder, Special Paper no. 349.

RAMOS, V. A. & FOLGUERA, A. 2009. Andean flat-slab subduction through time. In *Ancient Orogens and Modern Analogues* (eds J. B. Murphy, J. D. Keppie & A. J. Hynes), pp. 31–54. Geological Society of London, Special Publication no. 327.

RAMOS, V. A., JORDAN, T. E., ALLMENDINGER, R. W., MPODOZIS, C., KAY, S. M., CORTÉS, J. M. & PALMA, M. 1986. Paleozoic terranes of the Central Argentine–Chilean Andes. *Tectonics* **5**(6), 855–80.

RAMOS, V., MUNIZAGA, F. & KAY, S. M. 1991. El magmatismo cenozoico a los 33º S de latitud: geocronología y relaciones tectónicas. *6º Congreso Geológico Chileno*, Actas, Viña del Mar, pp. 892–96.

RAPELA, C. W., PANKHURST, R. J., CASQUET, C., BALDO, E., SAAVEDRA, J., GALINDO, C. & FANNING, C. M. 1998. The Pampean Orogeny of the southern proto-Andes: Cambrian continental collision in the Sierras de Córdoba. In *The Proto-Andean Margin of Gondwana* (eds R. J. Pankhurst & C. W. Rapela), pp. 181–217. Geological Society of London, Special Publication no. 142.

RAPELA, C. W., PANKHURST, R. J., CASQUET, C., FANNING, C. M., BALDO, E. G., GONZALEZ-CASADO, J. M., GALINDO, C. & DAHLQUIST, J. 2007. The Río de la Plata craton and the assembly of SW Gondwana. *Earth Science Review* **83**, 49–82.

RICHARDSON, T., RIDGWAY, K. D., GILBERT, H., MARTINO, R. D., ENKELMAN, E., ANDERSON, M. & ALVARADO, P. 2013. Neogene tectonics of the Eastern Sierras Pampeanas: active intraplate deformation inboard of flat-slab subduction. *Tectonics* **32**, 780–96.

RICHARDSON, T., RIDGWAY, K., MARTINO, R. D., GILBERT, H. J., ANDERSON, M. L., CARIGNANO, C. & ENKELMANN, E. 2009. Flat-slab subduction and continental deformation: an integrated geophysical and geological investigation of basement uplifts within the eastern Sierras Pampeanas, Argentina. *Transactions of EOS*, American Geophysical Union, Fall Meeting Supplement, Abstract T42B–06, San Francisco, California.

RODGERS, J. 1987. Chains of basement uplifts within cratons marginal to orogenic belts. *American Journal of Science* **287**, 661–92.

ROSSELLO, E. A. & MOZETIC, M. E. 1999. Caracterización estructural y significado geotectónico de los depocentros cretácicos continentales del centro-oeste argentino. *Boletim do 5º Simpósio o Cretáceo do Brasil*, 107–13, UNESP–Campus de Rio Claro/SP.

SCHLAGINTWEIT, O. 1954. Una interesante dislocación en Potrero de Garay (Valle de Calamuchita), Sierra Chica y Grande de la Provincia de Córdoba. *Revista de la Asociación Geológica Argentina* **9**, 135–54.

SCHMIDT, C. J., ASTINI, R. A., COSTA, C. H., GARDINI, C. E. & KRAEMER, P. E. 1995. Cretaceous rifting, alluvial fan sedimentation, and neogene inversion, Southern Sierras Pampeanas, Argentina. In *Petroleum Basins of South America* (eds A. J. Tankard, R. S. Suárez & H. J Welsink), pp. 341–58. American Association of Petroleum Geologists, Tulsa, Memoir no. 62.

SCHMIEDER, O. 1921. Apuntes geomorfológicos de la Sierra Grande de Córdoba. *Boletín de la Academia Nacional de Ciencias* **35**, 183–204. Córdoba.

SIEGESMUND, S., STEENKEN, A., MARTINO, R., WEMMER, K., LÓPEZ DE LUCHI, M., FREI, R., PRESNYAKOV, S. & GUERESCHI, A. 2010. Time constraints on the tectonic evolution of the Eastern Sierras Pampeanas (Central Argentina). *International Journal of Earth Sciences (Geologische Rundschau)* **99**, 1199–226.

SIMPSON, C., WHITMEYER, S., DE PAOR, D. G., GROMET, L. P., MIRO, R., KROL, M. A. & SHORT, H. 2001. Sequential ductile through brittle reactivation of major fault zones along the accretionary margin of Gondwana in Central Argentina. In *The Nature and Tectonic*

Significance of Fault Zone Weakening (eds R. E. Holdsworth, R. A. Strachan, M. J. F. & R. J. Knipe), pp. 233–55. Geological Society of London, Special Publications no. 186.

SNYDER, D. B., RAMOS, V. A. & ALLMENDINGER, R. W. 1990. Thick-skinned deformation observed on deep seismic reflection profiles in Western Argentina. *Tectonics* **9**, 773–88.

STEENKEN, A., WEMMER, K., MARTINO, R. D., LÓPEZ DE LUCHI, M. G., GUERESCHI, A. B. & SIEGESMUND, S. 2010. Post-Pampean cooling and the uplift of the Sierras Pampeanas in the west of Córdoba (Central Argentina). *Neues Jahrbuch für Geologie und Paläontologie–Abhandlungen* **256**, 235–55.

STELZNER, A. 1875. Comunicaciones sobre la geología y mineralogía de la República Argentina. Actas Academia Nacional de Ciencias de Córdoba, Tome I. Also in Anales del Ministerio de Agricultura de la República Argentina, Buenos Aires. Tome I, 1873 & Tome II, 1874, pp. 1–12.

STEWART, I. S. & HANCOCK, P. L. 1990. What is a fault scarp? *Episodes* **13**, 256–63.

TANKARD, A. J., ULIANA, M. A., WELSINK, H. J., RAMOS, V. A., TURIC, M., FRANÇA, A. B., MILANI, E. J., BRITO NEVES, B. B., EYLES, N., SKARMETA, J., SANTA ANA, H., WIENS, F., CIRBIÁN, M., LÓPEZ PAULSEN, O., GERMS, G. J. B., DE WIT, M. J., MACHACHA, T. & MILLER, R. 1995. Tectonic controls of basin evolution in southwestern Gondwana. In *Petroleum Basins of South America* (eds A. J. Tankard, R. Suárez Soruco & H. J. Welsink), pp. 5–52. American Association of Petroleum Geologists, Tulsa, Memoir no. 62.

ULIANA, M. A., BIDDLE, K. T. & CERDAN, J. 1989. Mesozoic extension and deformation of Argentine sedimentary basins. In *Extensional Tectonics and Stratigraphy in the North Atlantic Margin* (eds A. J. Tankard & H. R. Balkwill), pp. 599–614. American Association of Petroleum Geologists, Tulsa, Memoir no. 46.

VAN DER MEIJDE, M., JULIÀ, J. & ASSUMPÇÃO, M. 2013. Gravity derived Moho for South America. *Tectonophysics* **609**, 456–67.

WHITMEYER, S. 2008. Dating fault fabrics using modern techniques of $^{40}Ar/^{39}Ar$ thermochronology: evidence for Paleozoic deformation in the Eastern Sierras Pampeanas, Argentina. In *Making Sense of Shear* (ed. D. De Paor). *Journal of the Virtual Explorer* 30, paper no. 3, doi:10.3809/jvirtex.2008.00207.

YÁÑEZ, G. A., RANERO, C. R., VON HUENE, R. & DÍAZ, J. 2001. Magnetic anomaly interpretation across the southern central Andes (32°–34° S): The role of the Juan Fernández Ridge in the late Tertiary evolution of the margin. *Journal of Geophysical Research* **106**(B4), 6325–45.